

Deconvolution density estimation with penalised MLE

Yun Cai Hong Gu*

Toby Kenney†

Department of Mathematics and Statistics, Dalhousie University

May 25, 2021

Abstract

Deconvolution is the important problem of estimating the distribution of a quantity of interest from a sample with additive measurement error. Nearly all methods in the literature are based on Fourier transformation because it is mathematically a very neat solution. However, in practice these methods are unstable, and produce bad estimates when signal-noise ratio or sample size are low. In this paper, we develop a new deconvolution method based on maximum likelihood with a smoothness penalty. We show that our new method has much better performance than existing methods, particularly for small sample size or signal-noise ratio.

Keywords: deconvolution; penalised maximum likelihood estimation; density estimation; measurement error

1 Introduction

Measurement error is a common problem with data. It occurs when the apparatus measuring a variable is not perfect, and the value it returns is a random variable, based on the true value. A simple example is additive measurement error, where the recorded value is the true value (which is itself a random variable) plus a random error. More formally, the observed value is given by $Y = X + E$, where X is the true value and E is a random measurement error. This can happen with a lot of measurement apparatus. It can also happen when Y is an estimated quantity (such as an MLE estimate from a particular model on some data) for which there is no analytic solution. In this case, the estimates Y are subject to convergence error, which behaves like measurement error.

In this paper, we look at the problem of estimating the density of the underlying variable X from a sample of observations with measurement error. This is referred to as deconvolution. Figure 1 shows an example of this problem. The green curve is the density function of interest: it follows a scaled chi-squared distribution with 4 degrees of freedom. The black curve is the density of variable Y with measurement error following a scaled beta distribution. We see that the distribution with measurement error is very different from the original distribution, so some method is needed to correct for this difference.

Formally, we have a sample of observations Y_1, \dots, Y_n given by the additive error model $Y_j = X_j + \epsilon_j$, where ϵ_j are i.i.d. The latent variables X_j are i.i.d. with density f_x , but are not

*The authors gratefully acknowledge funding from NSERC

†The authors gratefully acknowledge funding from NSERC

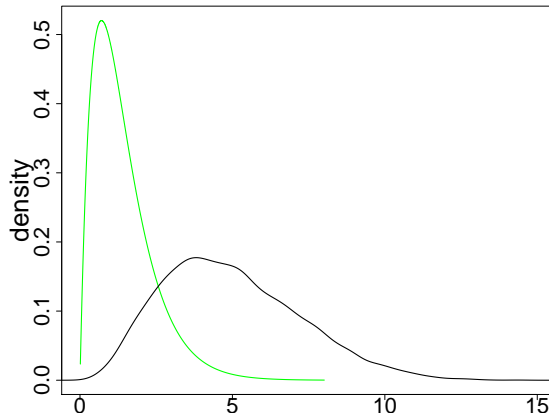


Figure 1: The black curve is the density of the contaminated data. The green curve is the density of the underlying truth.

observed. We are interested in estimating the density f_x from this data, and either a known error distribution for ϵ_j , or a separate sample from the error distribution (for example obtained by repeated measurements of one observation).

There have been a number of methods developed for this problem, almost all based on the characteristic function $\chi_X(t) = \mathbb{E}e^{iX}$. The key to the methods is that the convolution that gives the distribution of Y becomes pointwise multiplication of characteristic functions. That is, if Y has distribution function given by the convolution $F_Y(y) = \int_{-\infty}^{\infty} f_x(x)F_{\epsilon}(y-x) dx$, then the characteristic function is given by elementwise multiplication $\chi_Y(t) = \chi_X(t)\chi_{\epsilon}(t)$. Elementwise multiplication is easily inverted by elementwise division, i.e. $\chi_X(t) = \frac{\chi_Y(t)}{\chi_{\epsilon}(t)}$, so if we know the characteristic functions of Y and ϵ , then we can calculate the characteristic function of X . Different deconvolution methods in the literature are based on different estimators for the characteristic function of Y (and sometimes ϵ), and different regularisation and correction (the estimated χ_X is not guaranteed to be the characteristic function of a distribution). This formulation in terms of the characteristic function also highlights the difficult cases — when $\chi_{\epsilon}(t)$ is very small, the quotient becomes much larger, so estimation errors in the characteristic function are magnified. In cases where $\chi_{\epsilon}(t)$ converges quickly to zero as $t \rightarrow \infty$, the error distribution is called supersmooth, and the deconvolution problem is particularly challenging.

One widely used method is by Liu and Taylor (1989). They use a kernel density estimator for the characteristic function χ_Y , a known error distribution, and a method based on minimising mean squared error (MSE) to select the boundary and bandwidth. They prove the method is consistent in cases where the error distribution and kernel function are symmetric.

Assuming the error distribution as known is unrealistic. A more reasonable approach is to model the error distribution parametrically or nonparametrically. Delaigle and Gijbels (2004) used the moment estimators for the parametric error distribution parameters in their example, with the main contribution of the paper being a bootstrap bandwidth selection method for the deconvolution kernel density estimation of f_x . The R package `decon` (Wang and Wang, 2011) implements their method for Gaussian or Laplace error, using either direct computation or a fast Fourier transform (FFT).

The error distribution can be nonparametrically estimated from repeated observations of the contaminated variable Y , see for example, Delaigle et al. (2008) and Comte et al. (2014). Alternatively it can be estimated from a pure error sample (which can be obtained through repeated measurements of the same quantity which is independent of the observed sample of Y). For example, Kerkycharian et al. (2011) used the empirical characteristic function from a pure error sample for estimating χ_ϵ . There are a few other approaches to deconvolution with a pure error sample, mainly differing in details such as bandwidth selection.

The R package `deamer` (Stirnemann et al., 2012) implements several deconvolution methods based on the FFT algorithm, including situations for known error density; for unknown error density with an auxiliary sample of i.i.d. pure errors (method by Comte and Lacour (2011)) which is only proven consistent under the assumption that f_x is ordinary smooth or supersmooth; and for unknown error density with replicate observations for variable Y with the assumption that the error distribution is symmetric around zero (methods by Delaigle et al. (2008) and Comte et al. (2014)).

While the Fourier-based methods are mathematically elegant, estimation of the characteristic function is much more challenging than estimation of other distributional quantities, and because of the division by $\chi_\epsilon(t)$, values where $\chi_\epsilon(t)$ is small can cause instability in the estimates. The methods in the literature get around this by limiting the range of t . This hard limitation can result in poor estimation. Another source of significant errors comes in the correction stage where the estimate $\hat{\chi}_X(t) = \frac{\hat{\chi}_Y(t)}{\hat{\chi}_\epsilon(t)}$ is adjusted to become the characteristic function of a distribution. Because of these difficulties, existing methods perform very poorly unless the sample size and the signal-noise ratio (SNR) are both large.

In this paper, we develop a completely new method based on maximising the log-likelihood of the data plus a smoothness penalty on f_x , similar to the penalty used in smoothing splines. This method can overcome the difficulties with the Fourier-based methods, and produce better estimates, particularly when the sample size is small, or the SNR is low.

The outline of our paper is as follows. In Section 2, we introduce our method and define the estimator. In Section 3, we deal with the difficult computational challenges of the estimator. We discuss the theoretical convergence properties of our method in Section 4, with proofs in the appendix. In Section 5, we compare penalised MLE with `decon` and `deamer` on simulated datasets. In Section 6, we apply our method to real data and compare the performance with `decon` and `deamer`. The paper finishes with the conclusions in Section 7.

2 Deconvolution based on penalised log-likelihood

We want to estimate the density function $f_x(x)$ of the continuous random variable X from a sample $\{y_1, y_2, \dots, y_n\}$ of the random variable $Y = X + \epsilon$, where ϵ is another random variable. For simplicity, we will start with the case where the distribution of ϵ is known. If the distribution of ϵ is unknown, but we have a pure error sample, $\{e_1, e_2, \dots, e_M\}$, then we may apply our method with the empirical distribution of ϵ from this sample. We will also assume that X has finite support $[l, u]$. In theory, we could set the support to be $(-\infty, \infty)$, but this causes practical challenges with the optimisation.

The density function f_y is obtained via the convolution

$$f_y(y) = \mathbb{E}_\epsilon(f_x(y - \epsilon))$$

so the log-likelihood of our data for a particular density function f_x is

$$\sum_{i=1}^n \log f_y(y_i) = \sum_{i=1}^n \log \left(\int_l^u f_x(x) d\mu_\epsilon(y_i - x) \right)$$

where μ_ϵ is the probability measure of the error distribution. (We need to assume that X has a continuous distribution, but our method has no problems with ϵ having a discrete or mixed distribution.)

Our method is to minimise the negative log-likelihood function of $\{y_1, y_2, \dots, y_n\}$ plus a penalty term on the smoothness of function f_x . The smoothness penalty $\psi(f_x)$ is given by

$$\psi(f_x) = \langle f_x'', f_x'' \rangle = \int_l^u f_x''(x)^2 dx$$

where $\langle \cdot, \cdot \rangle$ denotes the inner product on the Hilbert space $L^2[l, u]$. This penalty is widely used in the smoothing splines method (Green and Silverman, 1993). This gives us the penalised negative log-likelihood function:

$$J = - \sum_{i=1}^n \log \left(\int_l^u f_x(x) d\mu_\epsilon(y_i - x) \right) + \lambda_n \langle f_x'', f_x'' \rangle \quad (1)$$

where λ_n is the smoothness penalty tuning parameter used to control the smoothness of f_x . To minimise J , we will rewrite the log-likelihood term by integrating by parts twice, to express the log-likelihood as a function of f_x'' . We can then solve for the optimal function f_x'' and obtain f_x by integrating twice.

Using integration by parts twice to compute the integral defining $f_y(y_i)$, we get

$$\begin{aligned} f_y(y_i) &= \int_l^u f_x(x) d\mu_\epsilon(y_i - x) \\ &= [-f_x(x)F_\epsilon(y_i - x)]_l^u + \int_l^u F_\epsilon(y_i - x) f_x'(x) dx \\ &= [-f_x(x)F_\epsilon(y_i - x)]_l^u - [f_x'(x)H(y_i - x)]_l^u + \int_l^u f_x''(x)H(y_i - x) dx \end{aligned} \quad (2)$$

where F_ϵ denotes the cumulative distribution function of f_ϵ and $H(v) = \int_{-\infty}^v F_\epsilon(u) du$.

We assume that f_x is a density function and $[l, u]$ contains the positive support of f_x , so without loss of generality we let $f_x(l) = f_x'(l) = 0$ and $f_x(u) = f_x'(u) = 0$. The first two terms in (2) vanish, giving

$$f_y(y_i) = \int_l^u f_x''(x)H(y_i - x) dx = \langle f_x'', h_i(x) \rangle$$

where $h_i(x) = H(y_i - x)$.

Using this inner product, our objective function (1) becomes

$$J = - \sum_{i=1}^n \log(\langle f_x'', h_i \rangle) + \lambda_n \langle f_x'', f_x'' \rangle \quad (3)$$

We want to minimise this J subject to the constraints:

$$f_x(l) = f_x'(l) = 0, \quad (4)$$

$$f_x(u) = f_x'(u) = 0, \quad (5)$$

$$\forall x \in (l, u), f_x(x) \geq 0, \quad (6)$$

$$\int_l^u f_x(x) dx = 1. \quad (7)$$

Constraint (4) gives a unique solution for f_x given f_x'' . The other conditions can be rewritten as conditions on f_x'' .

From (4) and (5), we get $\langle f_x''(x), x \rangle = 0$ and $\langle f_x''(x), 1 \rangle = 0$. From Constraints (4), (5) and (7) we get $\langle f_x''(x), x^2 \rangle = 2$. For the non-negativity constraint, (6), we integrate $f_x'(x)$ by parts to get the following inner products.

$$f_x(x) = \int_l^x f_x'(r) dr = [f_x'(r)(r-x)]_l^x - \int_l^x f_x''(r)(r-x) dr = \langle f_x''(r), (x-r)_+ \rangle \quad (8)$$

$$f_x(x) = - \int_x^u f_x'(r) dr = -[f_x'(r)(r-x)]_x^u + \int_x^u f_x''(r)(r-x) dr = \langle f_x''(r), (r-x)_+ \rangle \quad (9)$$

We can also take any affine combination of Equations (8) and (9) to evaluate $f_x(x)$. That is $f_x(x) = \lambda \langle f_x'', (x-r)_+ \rangle + (1-\lambda) \langle f_x'', (r-x)_+ \rangle$ for any λ . In particular, it is convenient to set $b_x(r) = \frac{(u-x)^2((u-x)+3(x-l))}{(u-l)^3} (x-r)_+ + \frac{(x-l)^2((x-l)+3(u-x))}{(u-l)^3} (r-x)_+ - 2 \frac{(u-x)^2(x-l)^2}{(u-l)^3}$, so that

$$\begin{aligned} \langle b_x, 1 \rangle &= \frac{(u-x)^2((u-x)+3(x-l))}{(u-l)^3} \int_l^x (x-r) dr + \frac{(x-l)^2((x-l)+3(u-x))}{(u-l)^3} \int_x^u (r-x) dr \\ &\quad - 2 \frac{(u-x)^2(x-l)^2}{(u-l)^3} \int_l^u 1 dr \\ &= \frac{1}{2} \left(\frac{(u-x)^2((u-x)+3(x-l))}{(u-l)^3} (x-l)^2 + \frac{(x-l)^2((x-l)+3(u-x))}{(u-l)^3} (u-x)^2 \right) - 2 \frac{(u-x)^2(x-l)^2}{(u-l)^2} \\ &= 0 \\ \langle b_x, r \rangle &= \langle b_x, r-x \rangle \\ &= \frac{(u-x)^2((u-x)+3(x-l))}{(u-l)^3} \int_l^x (r-x)(x-r) dr + \frac{(x-l)^2((x-l)+3(u-x))}{(u-l)^3} \int_x^u (r-x)(r-x) dr \\ &\quad - 2 \frac{(u-x)^2(x-l)^2}{(u-l)^3} \int_l^u (r-x) dr \\ &= \frac{1}{3} \left(- \frac{(u-x)^2((u-x)+3(x-l))}{(u-l)^3} (x-l)^3 + \frac{(x-l)^2((x-l)+3(u-x))}{(u-l)^3} (u-x)^3 \right) \\ &\quad - \frac{(u-x)^2(x-l)^2}{(u-l)^3} ((u-x)^2 - (x-l)^2) \\ &= \frac{(u-x)^2(x-l)^2}{(u-l)^3} \left(\frac{1}{3} (3(u-x)^2 - 3(x-l)^2) - ((u-x)^2 - (x-l)^2) \right) \\ &= 0 \end{aligned}$$

And the non-negativity constraint is $\langle f_x'', b_x \rangle \geq 0$ for all $x \in (l, u)$.

Thus we have converted the constraints in the minimisation problem from (3) to Hilbert Space inner product conditions on f_x'' :

$$J = - \sum_{i=1}^n \log(\langle f_x'', h_i \rangle) + \lambda_n \langle f_x'', f_x'' \rangle \quad (10)$$

$$\langle f_x'', 1 \rangle = 0 \quad (11)$$

$$\langle f_x'', x \rangle = 0 \quad (12)$$

$$\langle f_x'', x^2 \rangle = 2 \quad (13)$$

$$\langle f_x'', b_x \rangle \geq 0, \forall x \in (l, u) \quad (14)$$

The advantage of writing the optimisation problem in this way is that in the Hilbert space L^2 , we can decompose f_x'' as a linear combination of $\{h_i | i = 1, \dots, n\}$, $1, x, x^2$, and $\{b_x | x \in (l, u)\}$ plus a function orthogonal to all these elements. If we let f_0 be the linear combination of these elements, and let f_\perp be the orthogonal part, we see that f_\perp only affects the penalty term $\langle f_x'', f_x'' \rangle$, and because of the orthogonality, $\langle f_x'', f_x'' \rangle = \langle f_0, f_0 \rangle + \langle f_\perp, f_\perp \rangle$ is clearly minimised when $f_\perp = 0$, so we have shown that the optimal solution is a linear combination of $\{h_i | i = 1, \dots, n\}$, $1, x, x^2$, and $\{b_x | x \in (l, u)\}$. Thus, we have reduced the constrained optimisation over the whole Hilbert space $L^2((l, u))$ to a constrained optimisation of the coefficients in this basis. This is still infinite dimensional. However, we can get a good approximate solution to the problem by only requiring a finite subset of the non-negativity constraints. After we restrict to this condition, the problem has become a standard finite-dimensional constrained optimisation problem.

More precisely, suppose we choose $k - 3$ basis functions of $\{b_x | x \in (l, u)\}$, corresponding to $k - 3$ values for x , denoted by x_{n+4}, \dots, x_{n+k} , as constraint values, and want to minimise the objective function J subject to $f_x(l) = f_x'(l) = 0$, conditions (11)-(13) and condition (14) for $i = n + 4, \dots, n + k$. Let the basis functions be given by

$$k_i(r) = \begin{cases} h_i(r) & \text{if } i = 1, \dots, n \\ 1 & \text{if } i = n + 1 \\ r & \text{if } i = n + 2 \\ r^2 & \text{if } i = n + 3 \\ b_{x_i}(r) & \text{if } i = n + 4, \dots, n + k \end{cases} \quad (15)$$

From the above argument, we know that the solution to the optimisation problem is given by

$$f_x''(r) = \sum_{i=1}^{n+k} \alpha_i k_i(r) \quad (16)$$

for some coefficients $\alpha_1, \dots, \alpha_{n+k}$. If we form a matrix of inner products of these basis terms by

$$A_{ij} = \langle k_i, k_j \rangle \quad (17)$$

then the optimisation problem from Equations (10)–(14) can be rewritten as: Minimise

$$J = - \sum_{i=1}^n \log \left(\sum_{j=1}^{n+k} A_{ij} \alpha_j \right) + \lambda_n \sum_{i=1}^{n+k} \sum_{j=1}^{n+k} A_{ij} \alpha_i \alpha_j \quad (18)$$

subject to

$$\sum_{j=1}^{n+3} A_{(n+1)j} \alpha_j = 0 \quad (19)$$

$$\sum_{j=1}^{n+3} A_{(n+2)j} \alpha_j = 0 \quad (20)$$

$$\sum_{j=1}^{n+k} A_{(n+3)j} \alpha_j = 2 \quad (21)$$

$$(\forall i \in \{n+4, \dots, n+k\}) \sum_{j=1}^{n+k} A_{ij} \alpha_j \geq 0 \quad (22)$$

3 Practical Optimisation Issues

While the optimisation problem in Equations (18)–(22) looks like a fairly standard multidimensional optimisation problem, it is not completely straightforward. There are a number of choices that need to be made for the optimisation. Our implementation of the method uses the Nelder-Mead method (Nelder, 1965) in the `optim` function from the `stats` package in R. This is a simplex-based optimisation method. It has the advantage of being robust. This is particularly useful for our problem because the log-likelihood function is only defined for values of the parameters such that the convolved density is positive, so less robust methods sometimes produce invalid parameter values.

In addition to choice of optimisation method, there are a number of particular challenges present in this problem. In this section, we discuss the approach taken to deal with the following challenges: what values to set for l and u ; which non-negativity constraints to impose; initial values for parameters; computational singularity; and selection of tuning parameter.

3.1 Choosing l and u

In theory, as l and u tend to $-\infty$ and ∞ respectively, we should expect the solution to converge to the solution for support $(-\infty, \infty)$. However, in practice, ensuring the non-negativity constraints all hold becomes more difficult when the support is large and far from the observed data. Also, setting a narrower support reduces the computational difficulty of calculating the necessary inner products A_{ij} .

We initially set the support by first taking the empirical support l_Y, u_Y of the observed data points, and the empirical support l_e, u_e of the pure error sample. If the support of X is (l, u) and the support of ϵ is (l_e, u_e) , then the support of Y is $(l_Y, u_Y) = (l + l_e, u + u_e)$. Therefore, the support of X is given by $l = l_Y - l_e$ and $u = u_Y - u_e$. However, because it is easier to adjust the boundaries inward, and because we only have estimated values of l_Y, u_Y, l_e and u_e , we start with a wider interval than this.

When we fit the P-MLE for the initial support, it often happens that \hat{f}_x is negative near the boundaries and positive away from the boundaries. We then use an adaptive method to shrink the boundaries so that \hat{f}_x is positive on (l, u) . Suppose our current estimate for the support is (l_k, u_k) , and \hat{f}_x is negative on the interval (l_k, w_k) with a minimum at m_k , and on the interval (v_k, u_k) with a minimum at n_k . Then our next estimate for the support is $(\frac{l_k + m_k}{2}, \frac{n_k + u_k}{2})$.

3.2 Non-negativity constraints

To ensure the non-negativity of density function, a large number of constraints will be involved in the optimisation problem. This may cause numerical singularity of matrix A_{ij} and make the computational issues nontrivial. So for simplicity, we choose 30 evenly spaced points to cover the full range on the support of f_x . With the smoothness penalty, the estimated function will often be non-negative on the whole support.

3.3 Initial values

Random starting points are commonly used in many optimisation problems. However, in our case, random coefficients often do not produce valid density functions to satisfy the non-negative constraints. When the estimated density is negative somewhere, the log-likelihood cannot be computed. As a result, we need a better method to find the appropriate starting points. We take a kernel density estimate for f_Y as our starting point. We use a Gaussian kernel, with bandwidth estimated using Silverman’s rule-of-thumb (Silverman, 1986), in our implementation. We then project this estimated kernel density of f_Y orthogonally into the space spanned by our basis functions to get the initial coefficients. This can be easily achieved by evaluating the functions of f_Y and all basis functions at a large number of values over the support and solving a regression problem.

3.4 Computational Singularity

A large number of basis functions are translations of the function H . When H is a relatively smooth function, and when there are a lot of observed points, these translations can become close to be linearly dependent, which can cause numerically unstable solutions, or convergence problems and even sometimes incorrect results. We alleviate this problem using a subsampling approach on the basis. We choose a subsample of size S such that for a sample of S observation points, the translations h_i are not computationally singular. We then solve the optimisation problem for this subsample of basis elements (note that we use the whole data set to compute log-likelihood). In our experience, $S = 30$ usually works well. We repeat this for a number of subsamples, and average the results. To improve the reliability, the subsamples are stratified by dividing the support of Y into S intervals and selecting one sample point from each interval. This ensures that the subsample points are well spread-out, reducing the computational instability. We take enough subsamples to ensure that with high probability, the majority of basis elements have been used in at least one subsample. Even with this subsampling, it occasionally still happens that the optimisation fails for some subsamples. In these cases, a replacement subsample is drawn.

3.5 Selecting λ_n

The smoothness parameter λ_n needs to be selected. This is a tuning parameter, so the usual approach is via cross-validation. We divide the data into a training set and a validation set, use the training set to fit f_x , then evaluate the likelihood on the validation data, where the log-likelihood is $\sum_j \log((\hat{f}_x * \hat{f}_e)(y_j))$. We then choose λ_n to maximise this cross-validated log-likelihood.

In cases where computation time is limited, and we need to fit our method more quickly (for example in the simulations in Section 5), we have used the following heuristic approach to quickly select λ_n .

The role of λ_n is to find a reasonable balance between the log-likelihood and the smoothness penalty. For a given sample size, the right balance should be based on controlling the relative size of the two terms. Thus, we take the initial density estimate (before optimisation, since we need to choose λ_n before we can optimise) and compute the derivatives of the log-likelihood and derivatives of the smoothness penalty terms with respect to all the coefficients. We then set

$\lambda_n = \frac{1}{R} \frac{\sum_{i=1}^{n+k} \left| \frac{\partial l(f_{x;y})}{\partial \alpha_i} \right|}{\sum_{i=1}^{n+k} \left| \frac{\partial (f''_i, f''_i)}{\partial \alpha_i} \right|}$ for some constant R . From experience, we found that the following values for R work well.

Sample size	R
30	10^4
100	10^5
300	10^6

4 Theory

In this section, we discuss the theoretical large-sample performance of our method. For typical deconvolution problems, theoretical performance is controlled by the identifiability of the deconvolution problem. In particular, if one of the Fourier coefficients in the error distribution is zero, then the deconvolution problem is not identifiable, since adding the appropriate Fourier term to a “true” distribution does not change its convolution. In practice, distributions rarely have zero Fourier coefficients, so the method is not completely unidentifiable, but when the error distribution is super-smooth, then its Fourier coefficients quickly converge to zero, which makes the problem practically unidentifiable. We resolve this issue by studying the error in the convolved side, rather than the deconvolved side. That is, we can show that $\hat{f}_x * f_e \rightarrow f_y$ under general circumstances. This allows us to avoid worrying about ordinary smooth and super-smooth error distributions. We are able to show that P-MLE consistently produces a valid solution to the deconvolution problem. If there are multiple valid solutions, then the choice made by P-MLE may or may not be the truth. We are able to show that

Theorem 1 *Let the true density f_x be twice continuously differentiable, and let the convolved density be $f_y = f_x * f_e$. Let \hat{f}_x be the P-MLE estimate for f_x and $\hat{f}_y = \hat{f}_x * f_e$. If $\lambda_n = C_1 n^{\frac{7}{8}} \log(n)^{\frac{1}{8}} \sqrt{|u-l|}$, for a certain constant C_1 , then almost surely, for all sufficiently large n , $\|\hat{f}_y - f_y\|_\infty < C_2 n^{-\frac{1}{32}} |u-l|^{\frac{1}{8}} \log(n)^{\frac{1}{32}}$ for some constant C_2 . (The constants C_1 and C_2 depend on the smoothness $\psi(f_x)$ and $\psi(f_y)$ of the true distribution, but not on n , l , or u .)*

The details of this proof are in the supplementary appendix. Here, we briefly outline our approach.

1. By the Dvoretzky-Kiefer-Wolfowitz inequality (Dvoretzky et al., 1956), letting G denote the cumulative distribution function $G(t) = \int_{-\infty}^t f_y(s) ds$ and G_n denote the empirical distribution function of the sample y_1, \dots, y_n , the inequality

$$\|G_n - G\|_\infty \leq \sqrt{\frac{\log(n)}{n}} \tag{23}$$

almost surely holds for all sufficiently large n .

2. We construct a sequence of estimators f_n^* such that $\psi(f_n^*) < 2\psi(f_x)$, but the average likelihood $\frac{1}{n} \sum_{i=1}^n (f_n^* * f_e)(y_i)$ of the convolved density is bounded below by the negative entropy of the true data distribution minus a $O(n^{-\frac{1}{2}} \log(n)^{\frac{3}{2}})$ term.

3. We construct a sequence of estimators \tilde{g}_n from the data such that $\|\tilde{g}_n - f_y\|_\infty = O\left(\left(\frac{\log(n)}{n}\right)^{\frac{1}{4}}\right)$ and for any Lipschitz density g_L , the log-likelihood $\frac{1}{n} \sum_{i=1}^n g_L(y_i)$ is accurately approximated by $\int_I^u \tilde{g}_n(x) \log(g_L(x)) dx$.
4. Using the sequence \tilde{g}_n , we show that for any density function f , if $\|f * f_e - f_y\|_\infty > \rho_n$, for a suitably chosen $\rho_n \rightarrow 0$ then the penalised average log-likelihood of the data is smaller than the penalised average log-likelihood for the estimator \hat{f}_n . From this, we deduce that the P-MLE, \hat{f}_n must almost surely satisfy $\|\hat{f}_n * f_e - f_y\|_\infty \leq \rho_n$ for all sufficiently large n .

5 Simulations

In this section, we compare the performance of our method with two of the most popular methods in the literature: **deamer** (Stirnemann et al., 2012) and **decon** (Wang and Wang, 2011). For **decon**, we compare with both their methods with and without FFT. We compare the performance under a range of true and error distributions, including common examples from Comte and Lacour (2011) and Comte et al. (2006). We simulate with a range of different sample sizes and SNRs, including many cases with smaller sample size and SNR, which are often excluded from simulations in the literature, because they highlight a particular weakness of existing methods.

5.1 Simulation design

To cover a large range of scenarios of interest, we simulate all combinations from seven true distributions, three error distributions, three SNRs, and three sample sizes. The true distributions used in the simulation are:

Normal distribution.	$X \sim N(0, 1)$
Chi-square distribution.	$X \sim \chi^2(4)/\sqrt{8}$
Beta distribution.	$X \sim \sqrt{39.2}\text{Beta}(2, 5)$
Laplace distribution.	$f_x(x) = \frac{1}{\sqrt{2}} \exp(-\sqrt{2} x)$
Mixed normal distribution.	$X \sim \frac{2}{\sqrt{29}}(0.5N(-3, 1) + 0.5N(2, 1))$
Mixed gamma distribution.	$X \sim (0.4\Gamma(5, 1) + 0.6\Gamma(13, 1))/\sqrt{25.16}$
Cauchy distribution.	$f_x(x) = (1/\pi)/(1 + x^2)$

These distributions cover a range of situations including heavy tails, light tails, symmetric and skew distributions, unimodal and bimodal distributions, and different levels of smoothness. With the exception of the Cauchy distribution (which has infinite variance), these densities have all been normalised to have unit variance. These distributions have previously been used in the literature (Comte et al., 2006). However, the standardisation used in the literature was incorrect for the mixture distributions, so we have corrected the standardisation constants here.

For the error distribution, we use the following three distributions, scaled by a factor C . When the true distribution has finite variance (i.e. when it is not Cauchy), C^2 is the inverse of the SNR.

Laplace noise.	$f_\epsilon(\epsilon) = \frac{1}{\sqrt{2}} \exp(-\sqrt{2} \epsilon)$
Gaussian noise.	$f_\epsilon(\epsilon) = \frac{1}{\sqrt{2\pi}} \exp(-0.5\epsilon^2)$
Beta noise.	$f_\epsilon(\epsilon) = 30\sqrt{39.2}\epsilon(1 - \epsilon)^4$

We choose these three distributions because they have different levels of smoothness. The normal distribution is super smooth and the Laplace distribution is ordinary smooth. Both the normal distribution and the Laplace distribution are often used in the literature on measurement error. The beta distribution often arises as convergence error. The parameters of the three

distributions are chosen to ensure the error distribution has unit variance. Because the `decon` package only permits a limited number of chosen distribution families, which does not include the beta distribution, we were unable to compare its performance in the beta noise simulations.

In our simulation we study three sample sizes: 30, 100 and 300. In each case, we use the same sample size for the noisy data and for the pure error sample. Note, however, that because the `decon` package requires a known error distribution family, we provided the true error distribution to this package, which gives an unfair advantage to this method. This unfair advantage is particularly significant in the small sample size cases.

In each scenario, we simulate 100 replicates. For computational efficiency, we use the heuristic method from Section 3.5 to choose the smoothness penalty λ_n .

5.2 Simulation Results

We use Mean Integrated Squared Error (MISE) to evaluate the performance of the estimators in each scenario. This measure is defined by $MISE = E \int (\hat{f}_x(x) - f_x(x))^2 dx$. Here the MISE is computed as the empirical mean of the approximated ISE $\int (\hat{f}_x(x) - f_x(x))^2 dx$ over 100 simulation replicates. This is a traditional method for evaluating the performance of deconvolution methods that is widely used in the literature (Comte et al., 2006). We calculate the integral over an interval which contains both the support of the underlying true distribution from the 0.01% quantile to the 99.99% quantile and the estimated boundaries. `Deamer` does not give estimated boundaries for the true density, so we calculate its ISE on the same interval used for P-MLE. We numerically calculate the integral using the rectangle rule with the squared error evaluated at evenly-spaced points, where the spacing is chosen for each method so that there are 1000 (or 1024 for `decon` with FFT) points within the interval returned by the method. We found that changing the number of points used to estimate the ISE did not noticeably affect the results.

MISE for each method in each scenario is given in Tables 1–7. We see that P-MLE significantly outperforms both other methods in 153 out of 189 scenarios. `Deamer` significantly outperforms P-MLE in 16 out of 189 scenarios, and there are 14 scenarios where there is no significant difference between `deamer` and P-MLE. `Decon` does not significantly outperform P-MLE in any scenario, but there are 6 scenarios where P-MLE significantly outperforms `deamer` but not `decon`. Outperforming the state-of-the-art existing methods in such a wide range of scenarios is extremely impressive. It is also worth noting that because of the scale of the simulations, we used the heuristic approach to selecting the penalty parameter λ_n . For analysing a single data set, we would select λ_n more carefully using cross-validation, which would be expected to lead to better results. Furthermore, despite the fact that `decon` is using the true error distribution, while P-MLE and `deamer` are using an empirical estimate of the error distribution, `decon` never significantly outperforms P-MLE.

To see how much potential improvement could be made by choosing λ_n more carefully, we reran a number of scenarios where P-MLE was not the best method with a range of different values of λ_n . We found that in 6 of the 16 scenarios where `deamer` performed significantly better than P-MLE in the original results, another choice for λ_n using a different constant in the heuristic method would give an MISE that is not significantly different from `deamer`. In 2 more scenarios, different choices of λ_n improve results not significantly different from `deamer` to results that are significantly better than `deamer`. In one scenario, choosing a different constant for the heuristic choice of λ_n changes a result that is not significantly different from `decon` to a result that is significantly better. These results are based on choosing the value of λ_n which actually performs best for the scenario, rather than by cross-validation, so are not totally reliable. On the other hand, the results are using the heuristic approach, rather than tuning λ_n for each dataset, so it is possible that better tuning of λ_n might produce even better results. Full details of these

Table 1: MISE of the estimates when the underlying distribution is normal

The best overall performance in each simulation is highlighted in yellow if it is significantly better than other methods and in orange if the difference is not significant.

normal-normal		n=30		n=100		n=300	
		mean	se	mean	se	mean	se
SNR=4	P-MLE	0.0193	0.0015	0.0085	0.0007	0.0055	0.0004
	deamer	0.0486	0.0021	0.0097	0.0006	0.0029	0.0003
	decon	0.0286	0.0015	0.0147	0.0007	0.0082	0.0004
	decon (with FFT)	0.0283	0.0016	0.0151	0.0008	0.0081	0.0004
SNR=1	P-MLE	0.0232	0.0018	0.0121	0.0011	0.0068	0.0007
	deamer	0.1104	0.0025	0.0622	0.0014	0.0353	0.0004
	decon	0.0650	0.0023	0.0375	0.0012	0.0246	0.0008
	decon (with FFT)	0.0636	0.0018	0.0382	0.0012	0.0245	0.0009
SNR=0.25	P-MLE	0.0726	0.0025	0.0360	0.0019	0.0198	0.0021
	deamer	0.1973	0.0001	0.1782	0.0032	0.1247	0.0002
	decon	0.1066	0.0032	0.1039	0.0015	0.0839	0.0011
	decon (with FFT)	0.1073	0.0033	0.1030	0.0015	0.0836	0.0011
normal-laplace							
SNR=4	P-MLE	0.0187	0.0015	0.0072	0.0006	0.0046	0.0004
	deamer	0.0455	0.0019	0.0075	0.0005	0.0029	0.0003
	decon	0.0526	0.0052	0.0517	0.0062	0.0391	0.0050
	decon (with FFT)	0.0571	0.0064	0.0506	0.0065	0.0456	0.0057
SNR=1	P-MLE	0.0241	0.0017	0.0123	0.0009	0.0064	0.0008
	deamer	0.0974	0.0029	0.0462	0.0017	0.0156	0.0005
	decon	0.1083	0.0121	0.1142	0.0141	0.1010	0.0122
	decon (with FFT)	0.1125	0.0158	0.1222	0.0149	0.0902	0.0091
SNR=0.25	P-MLE	0.0682	0.0025	0.0412	0.0017	0.0217	0.0015
	deamer	0.1814	0.0030	0.1265	0.0015	0.0900	0.0026
	decon	0.2186	0.0263	0.2251	0.0236	0.2042	0.0185
	decon (with FFT)	0.2227	0.0295	0.2510	0.0378	0.2409	0.0280
normal-beta							
SNR=4	P-MLE	0.0307	0.0038	0.0157	0.0012	0.0145	0.0008
	deamer	0.0518	0.0020	0.0101	0.0057	0.0032	0.0002
SNR=1	P-MLE	0.0572	0.0049	0.0463	0.0022	0.0431	0.0021
	deamer	0.1111	0.0024	0.0641	0.0013	0.0411	0.0006
SNR=0.25	P-MLE	0.0824	0.0055	0.0515	0.0048	0.0414	0.0032
	deamer	0.1966	0.0008	0.1784	0.0317	0.1242	0.0002

Table 2: MISE of the estimates when the underlying distribution is chi-squared
The best overall performance in each simulation is highlighted in yellow if it is significantly better than other methods and in orange if the difference is not significant.

chisq-normal		n=30		n=100		n=300	
		mean	se	mean	se	mean	se
SNR=4	P-MLE	0.0453	0.0025	0.0268	0.0013	0.0175	0.0007
	deamer	0.0704	0.0025	0.0412	0.0012	0.0268	0.0006
	decon	0.0994	0.0024	0.0673	0.0014	0.0484	0.0008
	decon (with FFT)	0.1015	0.0023	0.0672	0.0014	0.0480	0.0009
SNR=1	P-MLE	0.0737	0.0028	0.0631	0.0024	0.0488	0.0015
	deamer	0.1424	0.0033	0.0993	0.0020	0.0750	0.0011
	decon	0.1429	0.0019	0.1050	0.0015	0.0830	0.0011
	decon (with FFT)	0.1435	0.0022	0.1034	0.0016	0.0826	0.0010
SNR=0.25	P-MLE	0.1412	0.0028	0.1037	0.0028	0.0706	0.0029
	deamer	0.2600	0.0024	0.2195	0.0034	0.1962	0.0002
	decon	0.1890	0.0030	0.1786	0.0013	0.1564	0.0010
	decon (with FFT)	0.1870	0.0027	0.1779	0.0013	0.1551	0.0011
chisq-laplace							
SNR=4	P-MLE	0.0446	0.0026	0.0260	0.0014	0.0144	0.0005
	deamer	0.0684	0.0027	0.0369	0.0009	0.0206	0.0006
	decon	0.0757	0.0060	0.0564	0.0058	0.0404	0.0036
	decon (with FFT)	0.0750	0.0060	0.0625	0.0066	0.0434	0.0039
SNR=1	P-MLE	0.0722	0.0025	0.0516	0.0018	0.0394	0.0011
	deamer	0.1244	0.0033	0.0773	0.0019	0.0505	0.0010
	decon	0.1322	0.0126	0.1318	0.0130	0.1357	0.0189
	decon (with FFT)	0.1377	0.0130	0.1321	0.0141	0.1151	0.0102
SNR=0.25	P-MLE	0.1314	0.0028	0.1035	0.0024	0.0781	0.0026
	deamer	0.2350	0.0039	0.1811	0.0026	0.1351	0.0017
	decon	0.2114	0.0170	0.2874	0.0279	0.2968	0.0354
	decon (with FFT)	0.2291	0.0210	0.2889	0.0280	0.3220	0.0340
chisq-beta							
SNR=4	P-MLE	0.0659	0.0040	0.0497	0.0044	0.0532	0.0034
	deamer	0.0702	0.0022	0.0423	0.0012	0.0279	0.0007
SNR=1	P-MLE	0.0874	0.0043	0.0727	0.0035	0.0895	0.0038
	deamer	0.1435	0.0027	0.0986	0.0019	0.0724	0.0010
SNR=0.25	P-MLE	0.1412	0.0054	0.0803	0.0047	0.0744	0.0048
	deamer	0.2632	0.0020	0.2137	0.0032	0.1948	0.0006

Table 3: MISE of the estimates when the underlying distribution is beta

The best overall performance in each simulation is highlighted in yellow if it is significantly better than other methods and in orange if the difference is not significant.

beta-normal		n=30		n=100		n=300	
		mean	se	mean	se	mean	se
SNR=4	P-MLE	0.0212	0.0015	0.0114	0.0007	0.0074	0.0004
	deamer	0.0328	0.0013	0.0168	0.0006	0.0096	0.0002
	decon	0.0646	0.0016	0.0395	0.0009	0.0257	0.0005
	decon (with FFT)	0.0717	0.0019	0.0405	0.0009	0.0262	0.0049
SNR=1	P-MLE	0.0341	0.0022	0.0248	0.0020	0.0158	0.0011
	deamer	0.0803	0.0023	0.0474	0.0013	0.0311	0.001
	decon	0.0987	0.0019	0.0621	0.0010	0.0439	0.0007
	decon (with FFT)	0.0987	0.0018	0.0616	0.0009	0.0443	0.0008
SNR=0.25	P-MLE	0.0821	0.0025	0.0456	0.0020	0.0359	0.0021
	deamer	0.1540	0.0027	0.1479	0.0029	0.1334	0.0002
	decon	0.1260	0.0029	0.1188	0.0012	0.0972	0.0009
	decon (with FFT)	0.1259	0.0028	0.1186	0.0010	0.0985	0.0009
beta-laplace							
SNR=4	P-MLE	0.0200	0.0014	0.0111	0.0007	0.0061	0.0003
	deamer	0.0319	0.0014	0.0154	0.0007	0.0082	0.0003
	decon	0.0560	0.0052	0.0458	0.0048	0.0374	0.0041
	decon (with FFT)	0.0605	0.0054	0.0472	0.0046	0.0334	0.0033
SNR=1	P-MLE	0.0327	0.0021	0.0191	0.0011	0.0127	0.0006
	deamer	0.0685	0.0022	0.0347	0.0014	0.0246	0.0007
	decon	0.1025	0.0010	0.1204	0.0132	0.1184	0.0114
	decon (with FFT)	0.1012	0.0103	0.1117	0.0121	0.1145	0.0011
SNR=0.25	P-MLE	0.0759	0.0024	0.0481	0.0016	0.0336	0.0016
	deamer	0.1656	0.0037	0.1147	0.0026	0.0758	0.0013
	decon	0.1973	0.0189	0.2305	0.0342	0.2657	0.0359
	decon (with FFT)	0.2081	0.0260	0.2104	0.0240	0.2778	0.0286
beta-beta							
SNR=4	P-MLE	0.0255	0.0021	0.0127	0.0007	0.0082	0.0006
	deamer	0.0336	0.0014	0.0172	0.0006	0.0097	0.0003
SNR=1	P-MLE	0.0501	0.0038	0.0386	0.0030	0.0316	0.0018
	deamer	0.0592	0.0023	0.0480	0.0014	0.0311	0.0010
SNR=0.25	P-MLE	0.0811	0.0042	0.0436	0.0031	0.0400	0.0026
	deamer	0.1944	0.0026	0.1437	0.0027	0.1292	0.0014

Table 4: MISE of the estimates when the underlying distribution is Laplace

The best overall performance in each simulation is highlighted in yellow if it is significantly better than other methods and in orange if the difference is not significant.

laplace-normal		n=30		n=100		n=300	
		mean	se	mean	se	mean	se
SNR=4	P-MLE	0.0441	0.0020	0.0282	0.0011	0.0282	0.0011
	deamer	0.1012	0.0024	0.0496	0.0008	0.0285	0.0003
	decon	0.0734	0.0016	0.0510	0.0011	0.0351	0.0008
	decon (with FFT)	0.0749	0.0020	0.0504	0.0012	0.0364	0.0007
SNR=1	P-MLE	0.0723	0.0024	0.0545	0.0020	0.0414	0.0015
	deamer	0.1767	0.0028	0.1267	0.0019	0.0955	0.0010
	decon	0.1247	0.0019	0.0920	0.0014	0.0728	0.0011
	decon (with FFT)	0.1260	0.0018	0.09231	0.0015	0.0746	0.0010
SNR=0.25	P-MLE	0.1343	0.0024	0.0969	0.0023	0.0548	0.0032
	deamer	0.2664	0.0013	0.2479	0.0033	0.1965	0.0007
	decon	0.1745	0.0035	0.1715	0.0016	0.1523	0.0013
	decon (with FFT)	0.1758	0.0035	0.1729	0.0015	0.1530	0.0011
laplace-laplace							
SNR=4	P-MLE	0.0427	0.0021	0.0250	0.0011	0.0157	0.0006
	deamer	0.0986	0.0027	0.0437	0.0010	0.0221	0.0004
	decon	0.0704	0.0062	0.0684	0.0084	0.0421	0.0044
	decon (with FFT)	0.0738	0.0070	0.0674	0.0084	0.0443	0.0046
SNR=1	P-MLE	0.0700	0.0026	0.0477	0.0018	0.0332	0.0014
	deamer	0.1576	0.0032	0.1030	0.0017	0.0658	0.0009
	decon	0.1283	0.0123	0.1485	0.0226	0.1006	0.0097
	decon (with FFT)	0.1287	0.0126	0.1256	0.0134	0.1023	0.0096
SNR=0.25	P-MLE	0.1332	0.0027	0.1021	0.0024	0.0673	0.0028
	deamer	0.2501	0.0032	0.1971	0.0013	0.1604	0.0027
	decon	0.2349	0.0279	0.3121	0.0427	0.2972	0.0294
	decon (with FFT)	0.2231	0.0194	0.2996	0.0446	0.3132	0.0330
laplace-beta							
SNR=4	P-MLE	0.0758	0.0042	0.0604	0.0036	0.0441	0.0036
	deamer	0.1040	0.0027	0.0520	0.0009	0.0293	0.0004
SNR=1	P-MLE	0.1068	0.0069	0.1100	0.0049	0.1361	0.0037
	deamer	0.1804	0.0026	0.1282	0.0017	0.0946	0.0010
SNR=0.25	P-MLE	0.1478	0.0059	0.1096	0.0064	0.1129	0.0063
	deamer	0.2667	0.0012	0.2534	0.0030	0.1952	0.0002

Table 5: MISE of the estimates when the underlying distribution is mixture-normal

The best overall performance in each simulation is highlighted in yellow if it is significantly better than other methods and in orange if the difference is not significant.

mixnormal-normal		n=30		n=100		n=300	
		mean	se	mean	se	mean	se
SNR=4	P-MLE	0.1145	0.0027	0.0780	0.0025	0.0412	0.0049
	deamer	0.1565	0.0019	0.1145	0.0018	0.0800	0.0016
	decon	0.1466	0.0015	0.1294	0.0008	0.1041	0.0009
	decon (with FFT)	0.1470	0.0016	0.1292	0.0008	0.1046	0.0008
SNR=1	P-MLE	0.1372	0.0022	0.1501	0.0048	0.1245	0.0040
	deamer	0.2108	0.0022	0.1642	0.0012	0.1388	0.0004
	decon	0.1695	0.0017	0.1465	0.0009	0.1365	0.0006
	decon (with FFT)	0.1681	0.0018	0.1464	0.0009	0.1368	0.0005
SNR=0.25	P-MLE	0.1724	0.0022	0.1456	0.0014	0.1800	0.0046
	deamer	0.2942	0.0010	0.2731	0.0034	0.2240	0.0007
	decon	0.2069	0.0030	0.2026	0.0012	0.1849	0.0010
	decon (with FFT)	0.2096	0.0032	0.2023	0.0014	0.1851	0.0010
mixnormal-laplace							
SNR=4	P-MLE	0.1085	0.0033	0.0646	0.0017	0.0462	0.0054
	deamer	0.1475	0.0024	0.0848	0.0025	0.0404	0.0014
	decon	0.1011	0.0066	0.0811	0.0073	0.0484	0.0043
	decon (with FFT)	0.1010	0.0055	0.0771	0.0058	0.0429	0.0041
SNR=1	P-MLE	0.1360	0.0021	0.1305	0.0032	0.0983	0.0045
	deamer	0.1986	0.0028	0.1524	0.0015	0.1252	0.0006
	decon	0.1735	0.0103	0.1575	0.0119	0.1249	0.0104
	decon (with FFT)	0.1802	0.0124	0.1555	0.0121	0.1206	0.0091
SNR=0.25	P-MLE	0.1674	0.0020	0.1486	0.0014	0.1531	0.0029
	deamer	0.2819	0.0029	0.2253	0.0012	0.1989	0.0026
	decon	0.3090	0.0307	0.3337	0.0341	0.3521	0.0281
	decon (with FFT)	0.3250	0.0312	0.3356	0.0383	0.3689	0.0317
mixnormal-beta							
SNR=4	P-MLE	0.1601	0.0041	0.1527	0.0030	0.1312	0.0026
	deamer	0.1561	0.0022	0.1159	0.0014	0.0747	0.0015
SNR=1	P-MLE	0.1747	0.0031	0.2095	0.0063	0.1921	0.0033
	deamer	0.2129	0.0021	0.1679	0.0008	0.1385	0.0004
SNR=0.25	P-MLE	0.1866	0.0033	0.1776	0.0032	0.1978	0.0034
	deamer	0.2951	0.0007	0.2812	0.0029	0.2281	0.0003

Table 6: MISE of the estimates when the underlying distribution is mixture-gamma

The best overall performance in each simulation is highlighted in yellow if it is significantly better than other methods and in orange if the difference is not significant.

mixgamma-normal		n=30		n=100		n=300	
		mean	se	mean	se	mean	se
SNR=4	P-MLE	0.0328	0.0016	0.0221	0.0009	0.0161	0.0008
	deamer	0.0412	0.0015	0.0258	0.0005	0.0209	0.0002
	decon	0.0756	0.0017	0.0458	0.0006	0.0335	0.0004
	decon (with FFT)	0.0795	0.0023	0.0460	0.0007	0.0338	0.0004
SNR=1	P-MLE	0.0381	0.0021	0.0362	0.0028	0.0267	0.0012
	deamer	0.0789	0.0024	0.0494	0.0012	0.0358	0.001
	decon	0.1020	0.0018	0.0655	0.0010	0.0500	0.0006
	decon (with FFT)	0.1012	0.0018	0.0656	0.0011	0.0497	0.0005
SNR=0.25	P-MLE	0.0780	0.0026	0.0469	0.0014	0.0462	0.0018
	deamer	0.1908	0.0029	0.1428	0.0026	0.1314	0.0005
	decon	0.1232	0.0028	0.1193	0.0011	0.0996	0.0085
	decon (with FFT)	0.1236	0.0027	0.1191	0.0010	0.0990	0.0094
mixgamma-laplace							
SNR=4	P-MLE	0.0321	0.0015	0.0210	0.0008	0.0133	0.0005
	deamer	0.0394	0.0013	0.0252	0.0005	0.0209	0.0002
	decon	0.0650	0.0052	0.0519	0.0059	0.0469	0.0041
	decon (with FFT)	0.0685	0.0070	0.0542	0.0068	0.0433	0.0039
SNR=1	P-MLE	0.0356	0.0017	0.0301	0.0011	0.0243	0.0013
	deamer	0.0698	0.0022	0.0418	0.001	0.0322	0.0005
	decon	0.1101	0.0119	0.1165	0.0146	0.0988	0.0104
	decon (with FFT)	0.1104	0.0118	0.1141	0.0114	0.1011	0.0110
SNR=0.25	P-MLE	0.0766	0.0023	0.0523	0.0016	0.0417	0.0019
	deamer	0.1599	0.0039	0.1140	0.0025	0.0873	0.0104
	decon	0.2709	0.0446	0.2323	0.0285	0.2764	0.0287
	decon (with FFT)	0.2998	0.0450	0.2382	0.0233	0.2703	0.0254
mixgamma-beta							
SNR=4	P-MLE	0.0423	0.0020	0.0315	0.0011	0.0246	0.0007
	deamer	0.0394	0.0012	0.0259	0.0005	0.0209	0.0002
SNR=1	P-MLE	0.0644	0.0030	0.0614	0.0029	0.0503	0.0016
	deamer	0.0802	0.0021	0.0505	0.0014	0.0420	0.0010
SNR=0.25	P-MLE 2	0.0884	0.0041	0.0623	0.0035	0.0565	0.0022
	deamer	0.1927	0.0026	0.1403	0.0024	0.1344	0.0013

Table 7: MISE of the estimates when the underlying distribution is Cauchy

The best overall performance in each simulation is highlighted in yellow if it is significantly better than other methods and in orange if the difference is not significant.

cauchy-normal		n=30		n=100		n=300	
		mean	se	mean	se	mean	se
C=0.5	P-MLE	0.0294	0.0024	0.0142	0.0007	0.0100	0.0004
	deamer	0.0513	0.0012	0.0354	0.0014	0.0106	0.0003
	decon	0.0259	0.0018	0.1356	0.0581	0.417	0.1905
	decon (with FFT)	0.0244	0.0010	0.0187	0.0016	0.0196	0.0027
C=1	P-MLE	0.0389	0.0080	0.0153	0.0007	0.0092	0.0003
	deamer	0.0649	0.0013	0.0369	0.0008	0.0239	0.0004
	decon	0.0392	0.0014	0.0891	0.0031	0.4274	0.1606
	decon (with FFT)	0.0368	0.0010	0.0803	0.0064	0.0315	0.0056
C=2	P-MLE	0.0473	0.0032	0.0285	0.0010	0.0228	0.0007
	deamer	0.0944	0.0001	0.0903	0.0004	0.0658	0.0018
	decon	0.0512	0.0017	0.2189	0.0221	0.1551	0.0603
	decon (with FFT)	0.0505	0.0016	0.2281	0.0256	0.0494	0.0034
cauchy-laplace							
SNR=4	P-MLE	0.0308	0.0025	0.0135	0.0006	0.0104	0.0004
	deamer	0.0503	0.0012	0.0347	0.0016	0.0110	0.0005
	decon	0.0535	0.0050	0.0527	0.0053	0.0974	0.0325
	decon (with FFT)	0.0692	0.0077	0.0521	0.0047	0.0472	0.0061
SNR=1	P-MLE	0.0330	0.0048	0.0146	0.0006	0.0093	0.0004
	deamer	0.0631	0.0014	0.0337	0.0006	0.0202	0.0003
	decon	0.0850	0.0079	0.1286	0.0173	0.1124	0.0146
	decon (with FFT)	0.0833	0.0073	0.1294	0.014	0.1016	0.0096
SNR=0.25	P-MLE	0.0354	0.0016	0.0236	0.0009	0.0173	0.0009
	deamer	0.0934	0.0005	0.0695	0.0019	0.0523	0.0005
	decon	0.2115	0.0262	0.3083	0.1464	0.3148	0.0415
	decon (with FFT)	0.1822	0.0180	0.2157	0.0266	0.3105	0.0581
cauchy-beta							
SNR=4	P-MLE	0.0428	0.0041	0.0164	0.0007	0.0108	0.0004
	deamer	0.0783	0.0020	0.0357	0.0004	0.0108	0.0003
SNR=1	P-MLE	0.0557	0.0049	0.0297	0.0013	0.0217	0.0010
	deamer	0.0899	0.0017	0.0349	0.0007	0.0238	0.0004
SNR=0.25	P-MLE	0.0708	0.0062	0.0532	0.0022	0.0516	0.0011
	deamer	0.0914	0.0001	0.0901	0.0005	0.0620	0.0016

Table 8: Summary of outcomes for each scenario

A — P-MLE significantly outperforms both other methods.

B — P-MLE significantly outperforms **deamer** but not **decon**.

C — No significant difference between P-MLE and **deamer**.

D — **Deamer** significantly outperforms P-MLE.

Outcome		A	B	C	D
True distribution	Normal	20	0	4	3
	Chi-squared	23	0	2	2
	Beta	26	0	1	0
	Laplace	23	0	1	3
	Mixnormal	18	3	2	4
	Mixgamma	22	0	1	4
	Cauchy	21	3	3	0
Error distribution	Normal	55	5	2	1
	Laplace	58	1	3	1
	Beta	40	NA	9	14
SNR	$C = 0.5$	40	2	11	10
	$C = 1$	52	2	3	6
	$C = 2$	61	2	0	0
Sample size	30	56	4	3	0
	100	53	1	4	5
	300	44	1	7	11

improvements are in the supplemental appendices.

Table 8 gives a breakdown of these simulation outcomes. We see that P-MLE outperforms the other methods for all true distributions, but the level of outperformance is less when the true distribution is a mixture of normal distributions. This is not surprising, since the mixture of normal distributions is bimodal, so the smoothness penalty will be larger than for the other distributions. However, even in this more challenging case, P-MLE still outperforms the other methods in most scenarios. The distribution of the noise has a bigger influence, with **deamer** performing relatively better when the noise follows a beta distribution. SNR is another important factor, with P-MLE performing much better than the other methods in the low SNR case. Finally, P-MLE outperforms **deamer** and **decon** in more scenarios with low sample size.

We also compare the distribution of the integrated squared error (ISE) for the different methods in each scenario. Figure 2 compares boxplots of the ISE for the three methods for each combination of true and error distributions for the case where sample size=30 and $C = 1$. While there are some outliers, and sometimes large variance, the results in most cases are fairly consistent, rather than being caused by a few outliers where one method gives a very poor estimate. An exception to this is the case where the true distribution is Cauchy and the error is normal. We see that P-MLE generally produced slightly better estimates than **decon**, but there was one simulation where the estimate from P-MLE was very poor, with ISE about 0.8, causing the overall MISE to be larger for P-MLE than **decon**. For $C = 0.5$, the situation is less clear-cut, but there are several outliers for P-MLE, so for most simulations the results are much closer between P-MLE and **decon**. Similar boxplots for other scenarios are in the Supplemental Appendices, Figures S1–S8.

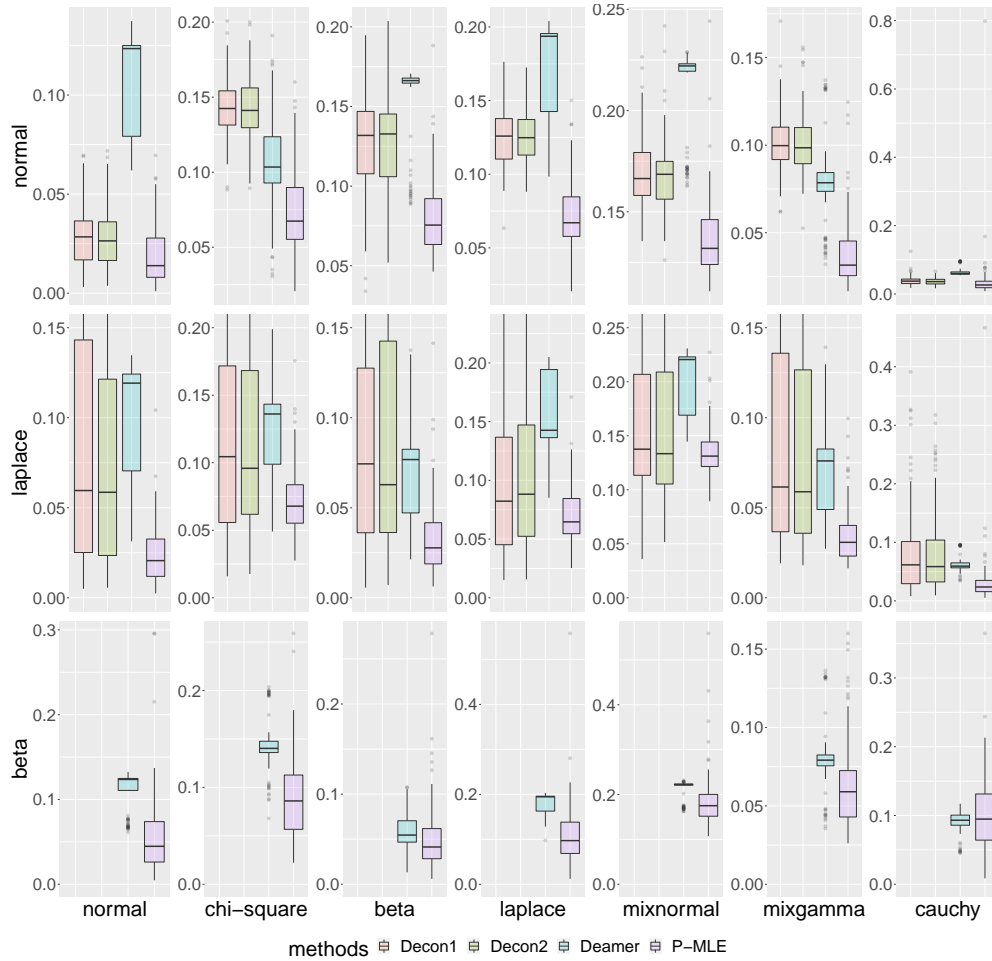


Figure 2: Sample distribution of ISE for sample size 30 and SNR 1. Each column corresponds to one of the seven true distributions in the simulation. Rows correspond to the error distribution. The `decon` package only allows a limited selection of error families, so could not be compared for simulations with a beta error. Some outliers where `decon` produced a large ISE are truncated from these plots. No P-MLE results have been truncated.

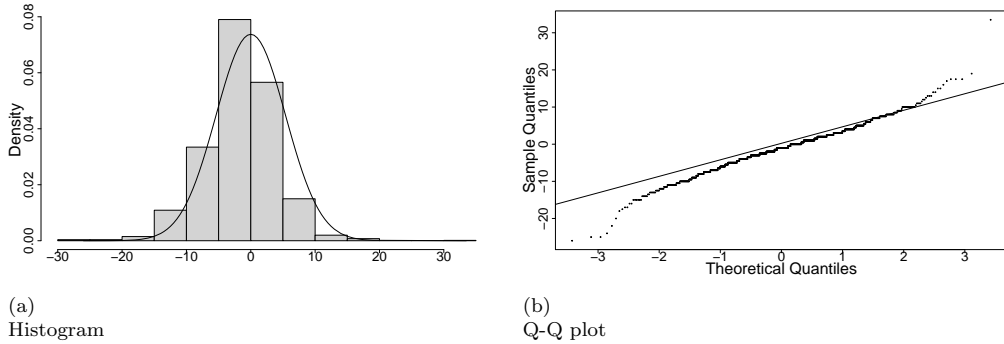


Figure 3: Comparison of real data error distribution with a normal distribution

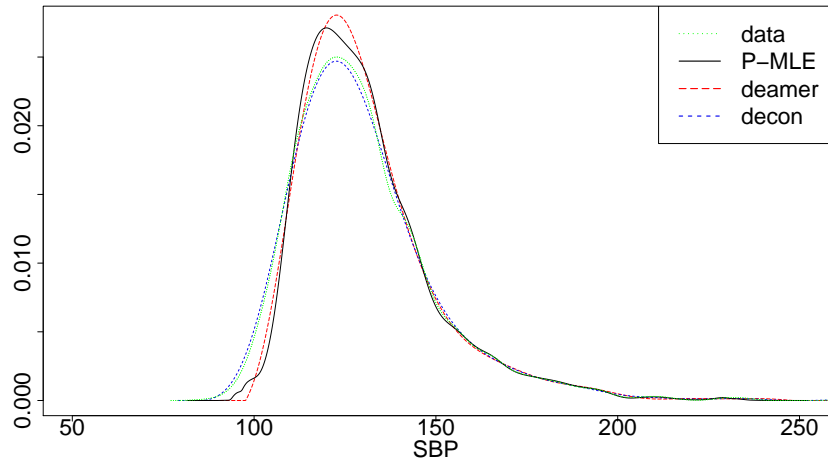
6 Real data analysis

Next we apply our P-MLE method to a real data set. The Framingham data (Carroll et al., 2006) records the systolic blood pressure measured for 1615 male subjects. Each subject’s blood pressure was measured twice at a first visit and twice at a second visit eight years later. We are going to use the measurements at the second visit only. Let SBP_{21} and SBP_{22} denote the two observations at the second visit. SBP_2 is the average of SBP_{21} and SBP_{22} . We are going to estimate the density of the underlying true blood pressure X from SBP_2 . We have $SBP_2 = X + e$, $e = \frac{e_{22} + e_{21}}{2}$. e_{21} and e_{22} are measurement errors of SBP_{21} and SBP_{22} . We also have $\frac{SBP_{22} - SBP_{21}}{2} = \frac{e_{22} - e_{21}}{2}$. Assume that the error distribution is symmetric, which is a common assumption for measurement error. Then $\frac{e_{22} + e_{21}}{2}$ and $\frac{e_{22} - e_{21}}{2}$ follow the same distribution. Therefore, we can use $\frac{SBP_{22} - SBP_{21}}{2}$ as the pure error sample for P-MLE and **deamer**. For **decon**, we assume the error distribution is normal with mean zero and estimated variance. Figure 3 shows the observed error distribution compared with an estimated normal density. We see that the normal assumption is not unreasonable for this distribution, though the error distribution appears to have heavier tails than the normal distribution.

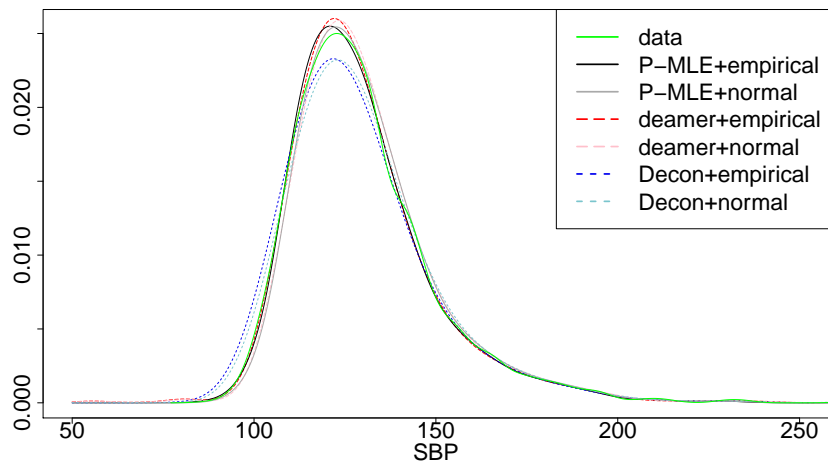
From the empirical distributions, the variance of the error sample is 29.274, and the variance of the observed sample is 395.6506. This suggests an SNR of about 12.5154.

Figure 4(a) shows the estimated true distributions by P-MLE and by **deamer** and **decon**. We see that P-MLE and **deamer** both select a much sharper peak and lower variance than the observed data, which is what we should expect to see, since adding noise should increase the variance and produce a less sharp peak. The density estimated by **decon** is extremely close to the observed data, suggesting that **decon** has not removed most of the measurement error.

To give a better sense of how well the methods estimate the latent true distribution, we convolve the estimated distributions with the error distribution and compare the results with a kernel density estimate from the observed data. Figure 4(b) compares the convolved estimated distribution for each method, convolving with both a normal measurement-error distribution, and the empirical error distribution. As can be seen, the distributions estimated by P-MLE and **deamer**, when convolved with the empirical error distribution, produce something close to the original data. **Decon** estimated a density much closer to the observed data, and as a result, the convolved estimator has higher variance than the observed data. We also see that when a normal error is used, the right tail of the distribution is estimated well by all methods, but the left tail is more challenging.



(a) Deconvolved estimate for density of distribution of SBP. A kernel density estimate of the observed values is shown for comparison, but this is with measurement error, so estimates close to the data estimate have not adequately removed the measurement error.



(b) Estimated density of SBP distribution convolved with error distribution, compared with a kernel density estimate from the observed data.

Figure 4: Real data results

Table 9: Difference between empirical distribution and convolved estimated distribution

	Normal Error			Empirical Error		
	A.D.	K.S.	ISE	A.D.	K.S.	ISE
P-MLE	2.632	0.0267	0.0135	0.778	0.0085	0.0051
Deamer	3.140	0.0302	0.0168	0.974	0.0071	0.0056
Decon	4.602	0.0228	0.0272	10.598	0.0412	0.0330
Decon (with FFT)	4.722	0.0237	0.0277	10.648	0.0414	0.0331

To give a quantitative measurement of the performance, we calculate the distance between the observed data and the estimated convolved distribution. We use both the Anderson-Darling (AD) distance and the Kolmogorov-Smirnov (KS) distance for measuring the difference. We also calculate the integrated squared difference between the estimated densities and the kernel density estimate from the real data in Figure 4(b). Because `deamer` and `decon` do not guarantee that the deconvolved “densities” returned have integral 1, we need to rescale them so that the AD and KS distances can be computed. We do not use Kullback-Leibler divergence because P-MLE directly optimises likelihood, so choosing a quantity so closely related to the objective function of P-MLE might be considered an unfair advantage to P-MLE, particularly considering that these results are on training data, so there is potential overfitting. The results are in Table 9. We see that, as expected, `decon` produces bad results, and that convolving with the empirical error distribution gives a closer result to the observed data than convolving with the normal distribution. For the empirical error distribution, `deamer` and P-MLE both perform similarly with P-MLE being better by some measures and `deamer` better under other measures. This is consistent with the simulation results, where for larger sample sizes, the difference in performance between `deamer` and P-MLE was small. We also see that the density functions estimated by P-MLE and `deamer` are quite different, but that the convolutions with the error density are much closer. This is the identifiability issue in the convolution problem, with two distributions having a very similar convolution with the measurement error distribution.

7 Conclusion

We have developed a deconvolution method for additive error based on penalised maximum log-likelihood estimation with a smoothness penalty on the estimated density. The smoothness penalty we use has previously been used to good effect in smoothing spline fittings. Our method is applicable to either continuous or discrete error distributions. In cases where the error distribution is unknown, this allows us to substitute the empirical distribution from a pure-error sample.

We have proved that our P-MLE method is consistent. We have also provided methods to address the practical optimisation difficulties which arise. In extensive simulation studies, and a real-data example, we have shown that our method has much better performance than existing methods, particularly when sample size and SNR are small. If faster computation is necessary, we provided a quick heuristic to choose the tuning parameter without cross-validation, and showed that with this heuristic, P-MLE produces good results, but with additional time to tune the penalty parameter λ_n by cross-validation, it will perform even better.

There are a number of directions in which the method can potentially be improved in future. Firstly, for practical purposes, we replaced the infinite number of non-negativity constraints by a finite subset of non-negativity constraints at a set of evenly spaced points. The solution to this constrained optimisation problem might not satisfy all the non-negativity constraints. It

seems likely that with carefully chosen constraints, we should be able to ensure that the estimated density satisfies all the non-negativity constraints. If this is the case, then it should be possible to develop an adaptive algorithm for choosing the correct points at which to impose non-negativity constraints.

Another issue that could be studied in the future is truncation. From the theory developed, we see that convergence depends upon the estimated support $|u - l|$ not increasing too fast as $n \rightarrow \infty$. For common light-tailed distributions, this will almost surely happen. However, for heavy-tailed distributions, the estimated support could grow too fast to achieve consistency. This problem could be resolved via an appropriate truncation method where certain data points are removed from the sample so that the rate of growth of the estimated support is controlled. This would be expected to improve large-sample performance in cases where the underlying true distribution is heavy-tailed. Given that P-MLE performed well in the Cauchy simulation results in Table 7, it seems that this is more of a theoretical issue than a practical concern.

References

- Carroll, R., Ruppert, D., Stefanski, L. and Crainiceanu, C. (2006) *Measurement Error in Non-linear Models: A Modern Perspective, Second Edition*. Chapman & Hall/CRC Monographs on Statistics & Applied Probability. CRC Press. URL: <https://books.google.ca/books?id=9kBx5CPZCqkC>.
- Comte, F. and Lacour, C. (2011) Data-driven density estimation in the presence of additive noise with unknown distribution. *Journal of the Royal Statistical Society: Series B (Statistical Methodology)*, **73**, 601–627.
- Comte, F., Rozenholc, Y. and Taupin, M.-L. (2006) Penalized contrast estimator for adaptive density deconvolution. *Canadian Journal of Statistics*, **34**, 431–452.
- Comte, F., Samson, A. and Stirnemann, J. J. (2014) Deconvolution estimation of onset of pregnancy with replicate observations. *Scandinavian Journal of Statistics*, **41**, 325–345.
- Delaigle, A. and Gijbels, I. (2004) Bootstrap bandwidth selection in kernel density estimation from a contaminated sample. *Annals of the Institute of Statistical Mathematics*, **56**, 19–47.
- Delaigle, A., Hall, P., Meister, A. et al. (2008) On deconvolution with repeated measurements. *The Annals of Statistics*, **36**, 665–685.
- Dvoretzky, A., Kiefer, J. and Wolfowitz, J. (1956) Asymptotic minimax character of the sample distribution function and of the classical multinomial estimator. *Ann. Math. Statist.*, **27**, 642–669.
- Green, P. J. and Silverman, B. W. (1993) *Nonparametric regression and generalized linear models: a roughness penalty approach*. Crc Press.
- Kerkycharian, G., Ngoc, T. M. P., Picard, D. et al. (2011) Localized spherical deconvolution. *The Annals of Statistics*, **39**, 1042–1068.
- Liu, M. C. and Taylor, R. L. (1989) A consistent nonparametric density estimator for the deconvolution problem. *Canadian Journal of Statistics*, **17**, 427–438.
- Nelder, John A. and Mead, R. (1965) A simplex method for function minimization. *The Computer Journal*, **7**, 13.

- Silverman, B. (1986) *Density Estimation for Statistics and Data Analysis*. Chapman & Hall/CRC. press.
- Stirnemann, J., Samson, A., Comte, F. and Lacour, C. (2012) Deconvolution density estimation with adaptive methods for a variable prone to measurement error. URL <https://cran.r-project.org/web/packages/deamer/index.html>. R package version, **1**.
- Wang, X.-F. and Wang, B. (2011) Deconvolution estimation in measurement error models: the r package decon. *Journal of statistical software*, **39**.

Supplementary Appendices to Deconvolution density estimation with penalized MLE

Yun Cai, Hong Gu & Toby Kenney

May 25, 2021

1 Theory

In this section we prove the consistency theorem from the main paper

Theorem 1.1. *Let the true density f_x be twice continuously differentiable, and let the convolved density be $f_y = f_x * f_e$. Let \hat{f}_x be the P-MLE estimate for f_x and $\hat{f}_y = \hat{f}_x * f_e$. If the smoothness penalty parameter for each estimate is given by $\lambda_n = C_1 n^{\frac{7}{8}} \log(n)^{\frac{1}{8}} \sqrt{|u-l|}$, for a certain constant C_1 , then almost surely, for all sufficiently large n , $\|\hat{f}_y - f_y\|_\infty < C_2 n^{-\frac{1}{32}} |u-l|^{\frac{1}{8}} \log(n)^{\frac{1}{32}}$ for some constant C_2 . The constants C_1 and C_2 are given by*

$$C_1 = \frac{2^{\frac{31}{20}} 3^{-\frac{1}{10}} 5^{\frac{3}{20}}}{\psi(f_x)^{\frac{4}{5}} \psi(f_y)^{\frac{1}{10}}}$$

$$C_2 = \left(1 + \sqrt{1 + \frac{3^{\frac{2}{5}}}{16}}\right)^{\frac{1}{4}} 2^{\frac{179}{80}} 3^{\frac{9}{40}} 5^{\frac{27}{80}} \psi(f_x)^{\frac{1}{4}} \psi(f_y)^{-\frac{1}{40}}$$

In this section, we will change the notation slightly to avoid excessive subscripts.

For a twice continuously differentiable function f with support S , let $\psi(f) = \int_S (f''(x))^2 dx$ be the smoothness penalty. Our estimator is the function \hat{f}_n that maximises the penalised log-likelihood.

$$\sum_{i=1}^n \log\left(\left(\hat{f}_n * f_e\right)(x_i)\right) - \lambda_n \psi\left(\hat{f}_n\right)$$

We want to prove consistency of \hat{f}_n . That is, more formally, suppose we have a sequence of i.i.d. observations x_1, x_2, \dots from a distribution with density function $f * f_e$, where f is twice differentiable with finite smoothness. We use the notation f_e for the density of the error distribution, but this is a slight abuse of notation, because the proof works equally well for non-continuous error distribution. Let $(\lambda_n)_{n=1, \dots}$ be a chosen sequence of penalty terms and $S_1 \subseteq S_2 \subseteq \dots$ be a chosen increasing sequence of measurable subsets of \mathbb{R} with union \mathbb{R} . Let \hat{f}_n be the twice continuous function with support S_n that maximises the penalised log-likelihood function

$$\sum_{i=1}^n \log\left(\left(\hat{f}_n * f_e\right)(x_i)\right) - \lambda_n \psi\left(\hat{f}_n\right)$$

for the first n observations. We want to prove that \hat{f}_n converges to f . Because of the difficulties that can arise when f_e is supersmooth, we will show that $\hat{f}_n * f_e$ converges to $f * f_e$. That is, we

will show that for some $\gamma, \xi > 0$, and some ζ , with probability 1, there is some N such that for all $n > N$ we have $\|(\hat{f}_n - f) * f_e\|_\infty < \gamma n^{-\xi} |S_n|^\zeta$.

In addition to the smoothness assumptions needed to state the problem, we will assume that $g = f * f_e$ has only a finite number M of local maxima. This eliminates a number of pathological distributions without eliminating any distributions of real interest. It simplifies the proof, but we believe that the method is still consistent without this assumption. This assumption is needed for Proposition 1.7, which allows a relatively simple proof of Proposition 1.16. However, we believe that a version of Proposition 1.16 (possibly with the lower bound changed slightly) is true without the need for this assumption.

In our proof, we will change between working on the noiseless scale of the underlying distribution we are trying to estimate, and working on the convolved scale, with the noise distribution added. We will consistently use f to represent densities on the noiseless scale, and g to represent densities on the convolved scale so for example $g = f * f_e$ refers to the convolved density of the true distribution. Similar notation will be used throughout. For example $\hat{g}_n = \hat{f}_n * f_e$ is the convolution of the penalised MLE estimate with the error distribution. For this proof, we will assume that f_e is known.

We will use the notation g for densities that are related to the convolved densities, even if they do not themselves arise as convolutions with f_e . For example, in the proof, we will introduce a density \tilde{g}_n , where we use the notation g because it is an estimator for the convolved density $g = f * f_e$, but the density \tilde{g}_n does not necessarily arise as a convolution of any density function with f_e .

To prove consistency, we will first note that the Dvoretzky-Kiefer-Wolfowitz (Dvoretzky et al., 1956) inequality gives that for any i.i.d. sample from a distribution with c.d.f. G , the c.d.f. G_n of the empirical distribution satisfies

$$P\left(\sqrt{n}\|G_n - G\|_\infty > \sqrt{\log(n)}\right) < Cn^{-2}$$

for some positive constant C (later, ? showed that $C = 1$), so the expected number of n for which

$$\|G_n - G\|_\infty > \sqrt{\frac{\log(n)}{n}}$$

is at most $C \sum_{i=1}^{\infty} n^{-2} < \infty$. Thus with probability 1, there is some N such that for all $n > N$ we have $\|G_n - G\|_\infty \leq \sqrt{\frac{\log(n)}{n}}$. In our case, we have that G is the c.d.f. for $g = f * f_e$, and G_n is the empirical c.d.f. of the observed sample.

Our approach for proving consistency will be as follows:

1. Construct a sequence of estimators $\tilde{g}_n(x)$ for g (we use kernel density estimators) such that the following conditions hold whenever $\|G_n - G\|_\infty \leq \sqrt{\frac{\log(n)}{n}}$.

(a) $\|\tilde{g}_n - g\|_\infty < C_3 \frac{\psi(g)^{\frac{1}{5}} \log(n)^{\frac{1}{4}}}{n^{\frac{1}{4}}}$ for some constant C_3 .

- (b) For any density function g_L^* that is Lipschitz with constant L and has support S_n , and has $g_L^*(x_i) \geq \epsilon$ for $i = 1, \dots, n$,

$$\left| \frac{1}{n} \sum_{i=1}^n \log(g_L^*(x_i)) - \int_{S_n} \tilde{g}_n(x) \log(g_L^*(x)) dx \right| < \frac{\log(n)^{\frac{1}{4}} L}{C_3 \psi(g)^{\frac{1}{5}} n^{\frac{1}{4}} \epsilon}$$

Intuitively, this is saying that the empirical mean of $\log(g_L^*(x))$ is close to the mean over the distribution \tilde{g} .

2. Construct a sequence of distributions f_n^* that converge to f , (based partly on the data, and partly on the true function f) with the following properties:

(a) $\psi(f_n^*) \leq 2\psi(f)$

(b) Whenever, $\|G_n - G\| < \sqrt{\frac{\log(n)}{n}}$, and n is sufficiently large, $\frac{1}{n} \sum_{i=1}^n \log(g_n^*(x_i)) > -H(g) - 4Mn^{-\frac{1}{2}} \log(n)^{\frac{3}{2}}$, where $H(g)$ is the entropy $-\int_{-\infty}^{\infty} g(x) \log(g(x))$.

3. Since the penalised likelihood of \hat{f}_n is bounded below by the penalised likelihood of f^* , using property 1(b), we can bound the likelihood of \hat{g}_n , which allows us to prove $\psi(\hat{f}_n) < 3\psi(f)$ for all sufficiently large n .

4. Having found a uniform Lipschitz constant for all \hat{g}_n , we will bound $\sum_{i=1}^n \log(\hat{g}_n(x_i))$ as a function of $\|\hat{g}_n - g\|_{\infty}$, and deduce that $\|\hat{g}_n - g\|_{\infty} \rightarrow 0$ almost surely.

1.1 Preliminary Results

We begin with some general inequalities and results about the smoothness penalty that will be necessary for proving our main results.

1.1.1 Smoothness and L^{∞} norms

Lemma 1.2. *If g is a density function, then $\psi(f * g) \leq \psi(f)$.*

Proof.

$$\begin{aligned}
\psi(f * g) &= \int_{-\infty}^{\infty} ((f * g)''(x))^2 dx \\
&= \int_{-\infty}^{\infty} \left(\frac{d^2}{dx^2} \int_{-\infty}^{\infty} g(t)f(x-t) dt \right)^2 dx \\
&= \int_{-\infty}^{\infty} \left(\int_{-\infty}^{\infty} g(t) \frac{d^2 f(x-t)}{dx^2} dt \right)^2 dx \\
&= \int_{-\infty}^{\infty} \left(\int_{-\infty}^{\infty} g(t)f''(x-t) dt \right) \left(\int_{-\infty}^{\infty} g(s)f''(x-s) ds \right) dx \\
&= \int_{-\infty}^{\infty} \int_{-\infty}^{\infty} g(t)g(s) \int_{-\infty}^{\infty} f''(x-t)f''(x-s) dx ds dt \\
&\leq \int_{-\infty}^{\infty} \int_{-\infty}^{\infty} g(t)g(s) \int_{-\infty}^{\infty} f''(x-t)^2 dx ds dt \\
&= \psi(f)
\end{aligned}$$

□

Remark 1.1. *It is straightforward to modify this proof in the case where the error distribution is not continuous.*

Lemma 1.3. *For any twice continuously differentiable density function g , $\|g\|_{\infty} \leq \left(\frac{5^4 \psi(g)}{3 \times 2^{12}} \right)^{\frac{1}{5}}$*

Proof. Suppose g attains its maximum at $x = 0$. (Since $\|g\|_\infty$ and $\psi(g)$ are translation invariant, there is no loss of generality). We first prove the result under the assumption that g is symmetric about 0.

For any constant $c > 0$, the function $h(x) = cg(cx)$ satisfies $\int_{-\infty}^{\infty} h(x) dx = \int_{-\infty}^{\infty} g(x) dx$, so h is a twice continuously differentiable density function. We have that $\|h\|_\infty = h(0) = cg(0) = c\|g\|_\infty$, and $h''(x) = c^3g''(cx)$, so $\psi(h) = c^5\psi(g)$. This means that $\|g\|_\infty\psi(g)^{-\frac{1}{5}} = \|h\|_\infty\psi(h)^{-\frac{1}{5}}$. Thus, in trying to maximise $\|g\|_\infty\psi(g)^{-\frac{1}{5}}$, we may without loss of generality assume that $\int_0^1 g(x) dx = 0.4g(0)$.

Let $m = \sup g(x) = g(0)$. Let $a = g(1)$, $b = g'(1)$. We have $\int_0^1 g(x) dx = 0.4m$, $g(0) = m$ and $g'(0) = 0$. Now on the Hilbert space $L^2([0, 1])$, we have

$$\begin{aligned}\langle g'', x^2 \rangle &= \int_0^1 x^2 g''(x) dx = [x^2 g'(x)]_0^1 - [2xg(x)]_0^1 + 2 \int_0^1 g(x) dx \\ &= b - 2a + 0.8m \\ \langle g'', x \rangle &= [xg'(x)]_0^1 - \int_0^1 g'(x) dx \\ &= b + m - a \\ \langle g'', 1 \rangle &= b \\ \langle x^\alpha, x^\beta \rangle &= \frac{1}{\alpha + \beta + 1}\end{aligned}$$

Clearly subject to these conditions, $\|g''\|_2$ is minimised by setting g'' to be a linear combination $\beta_0 + \beta_1 x + \beta_2 x^2$. Let $v = (\beta_0, \beta_1, \beta_2)^T$ and let

$$M = \begin{pmatrix} 1 & \frac{1}{2} & \frac{1}{3} \\ \frac{1}{2} & \frac{1}{3} & \frac{1}{4} \\ \frac{1}{3} & \frac{1}{4} & \frac{1}{5} \end{pmatrix}$$

Be given by $M_{ij} = \langle x^{i-1}, x^{j-1} \rangle$. Then our equations become $Mv = w$, where $w = (b, b + m - a, b - 2a + 0.8m)^T$. We have

$$M^{-1} = \begin{pmatrix} 9 & -36 & 30 \\ -36 & 192 & -180 \\ 30 & -180 & 180 \end{pmatrix}$$

Thus $\|g''\|_2^2 \geq v^T Mv = w^T M^{-1} M M^{-1} w = w^T M^{-1} w$. Let $t = (m, a, b)^T$. Then $w = Bt$ where

$$B = \begin{pmatrix} 0 & 0 & 1 \\ 1 & -1 & 1 \\ 0.8 & -2 & 1 \end{pmatrix}$$

This gives

$$\|g''\|_2^2 \geq t^T B^T M^{-1} B t = (m, a, b) \begin{pmatrix} 19.2 & 24 & 0 \\ 24 & 192 & -36 \\ 0 & -36 & 9 \end{pmatrix} \begin{pmatrix} m \\ a \\ b \end{pmatrix}$$

For fixed a , $\|g''\|_2$ is minimised when $b = 4a$. In this case $t^T B^T M^{-1} B t$ is an increasing function of a for all non-negative a . Since $a \geq 0$, $t^T B^T M^{-1} B t$ is minimised when $a = b = 0$. Thus $\|g''\|_2^2 \geq 19.2m^2$.

Now since g is an even function, we have $\int_{-1}^1 g(x) dx = 0.8m \leq 1$. It follows that $m \leq 1.25$ and $\psi(g) \geq 2t^T B^T M^{-1} B t \geq 38.4m^2 \geq \frac{38.4m^5}{1.25^3} = \frac{3 \times 2^{12}}{5^4} m^5$. Therefore, $\|g\|_\infty \psi(g)^{-\frac{1}{5}} \leq \left(\frac{5^4}{3 \times 2^{12}}\right)^{\frac{1}{5}}$.

We have proved the result when g is symmetric about 0. Suppose g is not symmetric about 0. Let $s_+(x) = \frac{g(|x|)}{c_+}$ and $s_-(x) = \frac{g(-|x|)}{c_-}$ be the symmetric density functions obtained by reflecting the positive and negative parts of g respectively in the y axis, and rescaling. The positive constants c_+ and c_- are chosen so that $\int_{-\infty}^{\infty} s_+(x) dx = 1$ and $\int_{-\infty}^{\infty} s_-(x) dx = 1$. That is, $c_- = 2 \int_{-\infty}^0 g(x) dx$ and $c_+ = 2 \int_0^{\infty} g(x) dx$. It is easy to see that s_+ and s_- are twice continuously differentiable density functions (because $g'(0) = 0$), and are symmetric, so applying the result for symmetric functions, we get $\psi(s_+) \geq \frac{3 \times 2^{12}}{5^4} \frac{\|g\|_\infty^5}{c_+^5}$ and $\psi(s_-) \geq \frac{3 \times 2^{12}}{5^4} \frac{\|g\|_\infty^5}{c_-^5}$. Also, we have $\psi(g) = \frac{1}{2} (c_-^2 \psi(s_-) + c_+^2 \psi(s_+)) \geq \frac{3 \times 2^{11}}{5^4} \|g\|_\infty^5 \left(\frac{1}{c_-^3} + \frac{1}{c_+^3}\right)$. Since $\int_{-\infty}^{\infty} g(x) dx = 1$, we have $c_- + c_+ = 2$, so $c_-^{-3} + c_+^{-3}$ is minimised when $c_- = c_+ = 1$. Thus, the result holds for any g . \square

Corollary 1.4. *For any density function f and any distribution, f_e , $\|f * f_e\|_\infty \leq \left(\frac{5^4 \psi(f)}{3 \times 2^{12}}\right)^{\frac{1}{5}}$*

Proof. This is immediate from Lemma 1.2 and Lemma 1.3 \square

Lemma 1.5. *If a density function $g : \mathbb{R} \rightarrow \mathbb{R}_{\geq 0}$ is twice continuously differentiable and has finite support, then $\|g'\|_\infty \leq \left(\frac{125\psi(g)^2}{144}\right)^{\frac{1}{5}}$*

Proof. Translating if necessary, we may assume that $|g'(x)|$ is maximised by $x = 0$. By reflecting in the line $x = 0$ if necessary, we may also assume $g'(0) > 0$. We may also rescale (that is, replace g by $h(x) = cg(cx)$ as in the proof of Proposition 1.3: it is easy to check that $\|g'\|_\infty \psi(g)^{-\frac{2}{5}} = \|h'\|_\infty \psi(h)^{-\frac{2}{5}}$) so that $g(1) = g'(1) = 0$. We will prove the result by finding a suitable function h that minimises $\psi(h)$ subject to the constraints

- (i) $\|h'\|_\infty = h'(0) = s > 0$
- (ii) $\int_{-\infty}^1 h(x) dx \leq 1$,
- (iii) h is twice continuously differentiable everywhere except for one value $x \leq 0$ at which $h(x) = 0$.

Since these conditions on h are slightly weaker than the conditions for g in the proposition, any g satisfying the conditions of the proposition also satisfies the conditions for h . It follows that $\psi(g)^{-\frac{2}{5}} \|g'\|_\infty \leq \psi(h)^{-\frac{2}{5}} \|h'\|_\infty$, so if this h satisfies the inequality in the proposition, the result will be proved.

Let

$$k(x) = \begin{cases} 0 & \text{if } x < -\frac{h(0)}{h'(0)} \\ h'(0)x + h(0) & \text{if } -\frac{h(0)}{h'(0)} \leq x < 0 \\ h(x) & \text{if } x \geq 0 \end{cases}$$

That is, k is a linear extension of the restriction of h to positive real numbers. By inspection, $\|k'\|_\infty \leq h'(0) = s$, so k satisfies Condition (i); also by the mean value theorem, $k(x) \leq h(x)$ for all x , so $\int_0^1 k(x) dx \leq \int_0^1 h(x) dx \leq 1$, so k satisfies Condition (ii). Finally, Condition (iii) is obvious on all intervals, $\left(-\infty, -\frac{h(0)}{h'(0)}\right]$, $\left(-\frac{h(0)}{h'(0)}, 0\right]$ and $(0, \infty)$, so the condition only needs to be tested at 0. At 0, we obviously have $k'(0) = h'(0) = s$, and $k''(0) = h''(0) = 0$ because $h'(x)$ attains its maximum value at $x = 0$.

Since k satisfies the same conditions as h , we have $\psi(k) \geq \psi(h)$. On the other hand $|k''(x)| \leq |h''(x)|$ for all x , so $\psi(k) \leq \psi(h)$. Therefore, $k\left(x + \frac{h(0)}{h'(0)}\right)$ is an alternative minimiser of $\psi(k)$ subject to Conditions (i)–(iii), and it satisfies the additional condition that $k(0) = 0$. Thus, we may assume w.l.o.g. that $h(0) = 0$.

Now since $h(0) = 0$, $h'(0) = s$, $h(1) = 0$, $h'(1) = 0$ and $\int_0^1 h(x) dx = r \leq 1$, we have

$$\begin{aligned}\langle h'', 1 \rangle &= \int_0^1 h''(x) dx = h'(1) - h'(0) = -s \\ \langle h'', x \rangle &= [h'(x)x]_0^1 - \int_0^1 h'(x) dx = h'(1) - (h(1) - h(0)) = 0 \\ \langle h'', x^2 \rangle &= [h'(x)x^2]_0^1 - 2[h(x)x]_0^1 + 2 \int_0^1 h(x) dx = 2r \leq 2\end{aligned}$$

It is easy to see that subject to these conditions, $\psi(h)$ is minimised by setting h'' as a linear combination of 1, x and x^2 . Let $h''(x) = a + bx + cx^2$. Then we have

$$\begin{pmatrix} 1 & \frac{1}{2} & \frac{1}{3} \\ \frac{1}{2} & \frac{1}{3} & \frac{1}{4} \\ \frac{1}{3} & \frac{1}{4} & \frac{1}{5} \end{pmatrix} \begin{pmatrix} a \\ b \\ c \end{pmatrix} = \begin{pmatrix} -s \\ 0 \\ 2r \end{pmatrix}$$

which gives

$$\begin{pmatrix} a \\ b \\ c \end{pmatrix} = \begin{pmatrix} 9 & -36 & 30 \\ -36 & 192 & -180 \\ 30 & -180 & 180 \end{pmatrix} \begin{pmatrix} -s \\ 0 \\ 2r \end{pmatrix}$$

and $\psi(h) = 9s^2 - 120sr + 720r^2$.

Recall that by rescaling, we are aiming to minimise

$$\psi(h) \|h'\|_{\infty}^{-\frac{5}{2}} = 9s^{-\frac{1}{2}} - 120rs^{-\frac{3}{2}} + 720r^2s^{-\frac{5}{2}}$$

It is easy to see that this is minimised when s is a solution to

$$\begin{aligned}-\frac{1}{2}9s^{-\frac{3}{2}} + 120\frac{3}{2}rs^{-\frac{5}{2}} - 720\frac{5}{2}r^2s^{-\frac{7}{2}} &= 0 \\ -s^2 + 40rs - 400r^2 &= 0 \\ s &= 20r\end{aligned}$$

For $s = 20r$, we have

$$\frac{\psi(h)^2}{s^5} = \frac{(3600 - 2400 + 720)^2 r^2}{20^5 r^5} = \frac{1920^2}{20^5 r^3} = \frac{144}{125} r^{-3}$$

Since $r \leq 1$, we deduce $\frac{\psi(h)^2}{\|h'\|_{\infty}^5} \leq \frac{144}{125}$.

□

1.1.2 General Inequalities and probability theory

We start by showing that for any random variable, there is at least one point at which it has positive density.

Lemma 1.6. *For any random variable E , there is some b , $\delta > 0$ and $\epsilon > 0$ such that for any $t < \delta$, $P(|E - b| < t) > \epsilon t$.*

Proof. Pick a finite interval $[l_0, u_0]$ such that E has finite probability p on the interval $[l_0, u_0]$, and let $d = \frac{p}{u_0 - l_0}$. Let m_0 be the midpoint of $[l_0, u_0]$, For the intervals $[l_0, m_0]$ and $[m_0, u_0]$, we have $P(E \in [l_0, m_0]) + P(E \in [m_0, u_0]) = p$, so one of $P(E \in [l_0, m_0])$ and $P(E \in [m_0, u_0])$ must be at least $\frac{p}{2}$. Without loss of generality, suppose $P(E \in [l_0, m_0]) \geq \frac{p}{2}$. We now let $l_1 = l_0$ and $u_1 = m_0$ to create a new interval whose average density is at least $\frac{p}{u_0 - l_0}$. Repeating this interval bisection, we get a decreasing sequence of intervals $[l_k, u_k]$ whose intersection is a single point b . We will show that this b with $\delta = (u_0 - l_0)$ satisfies the result. To do this, for any $t < \delta$, we will show that there is some k such that $[l_k, u_k] \subseteq [b - t, b + t]$ and $u_k - l_k > \frac{t}{2}$. It will follow that $P(|E - b| < t) \geq P(E \in [l_k, u_k]) \geq d(u_k - l_k) \geq d \frac{t}{2}$. For $t \geq \max(u_0 - b, b - l_0)$, $k = 0$ obviously satisfies the conditions. Otherwise, since $l_k \rightarrow b$ and $u_k \rightarrow b$, there must be some smallest k such that $[l_k, u_k] \subseteq [b - t, b + t]$. By minimality of this k , we have that either $l_{k-1} < b - t$ or $u_{k-1} > b + t$. In either case, $u_k - l_k = \frac{u_{k-1} - l_{k-1}}{2} > \frac{t}{2}$. \square

Proposition 1.7. *Let g be a twice continuously differentiable function with support $[l, u]$ and with at most M local maxima. Let $r > 0$ and set $b(x) = g(x) \vee r$. Then*

$$\int_l^u \left| \frac{b'(x)}{b(x)} \right| dx \leq \frac{2M}{5} \log \left(\frac{5^4 \psi(g)}{3 \times 2^{12} r^5} \right)$$

Proof. Let the local maxima of $g(x)$ be at $a_1 < a_3 < \dots < a_{2M-1}$, and let the local minima be at $a_2 < a_4 < \dots < a_{2M-2}$, and let $a_0 = l, a_{2M} = u$. We have

$$\begin{aligned} \int_l^u \left| \frac{b'(x)}{b(x)} \right| dx &= \sum_{i=0}^{M-1} \left(\int_{a_{2i}}^{a_{2i+1}} \frac{b'(x)}{b(x)} dx - \int_{a_{2i+1}}^{a_{2i+2}} \frac{b'(x)}{b(x)} dx \right) \\ &= \sum_{i=0}^{M-1} (2 \log(b(a_{2i+1})) - \log(b(a_{2i})) - \log(b(a_{2i+2}))) \\ &\leq 2 \sum_{i=0}^{M-1} \log \left(\frac{b(a_{2i+1})}{r} \right) \end{aligned}$$

By Lemma 1.3, we have $\|g\|_\infty \leq \left(\frac{5^4 \psi(g)}{3 \times 2^{12}} \right)^{\frac{1}{5}}$, so $\log(b(a_{2i+1})) \leq \log \left(\left(\frac{5^4 \psi(g)}{3 \times 2^{12}} \right)^{\frac{1}{5}} \right)$ This gives

$$\int_l^u \left| \frac{b'(x)}{b(x)} \right| dx \leq \frac{2M}{5} \log \left(\frac{5^4 \psi(g)}{3 \times 2^{12} r^5} \right)$$

\square

1.1.3 Kulback-Leibler Divergence

Lemma 1.8. *If g and h are density functions and $h(x) > g(x) + \epsilon$ for all $x \in [x_0 - \delta, x_0 + \delta]$, then the Kulback-Leibler divergence is bounded below by $\int g(x) \log \left(\frac{g(x)}{h(x)} \right) dx > 2\delta^2 \epsilon^2$*

Proof. Let $h(x) = k(x) + l(x)$, where

$$l(x) = \begin{cases} \epsilon & \text{if } |x - x_0| < \delta \\ 0 & \text{otherwise} \end{cases}$$

Since $h(x) > g(x) + \epsilon$ for all $x \in [x_0 - \delta, x_0 + \delta]$, it follows that $k(x) > g(x)$ for all $x \in [x_0 - \delta, x_0 + \delta]$.

Now $\log(h(x)) = \log(k(x)) + \log\left(1 + \frac{l(x)}{k(x)}\right)$, so

$$\begin{aligned} \int g(x) \log(h(x)) dx &= \int g(x) \log(k(x)) dx + \int_{x_0 - \delta}^{x_0 + \delta} g(x) \log\left(1 + \frac{\epsilon}{k(x)}\right) dx \\ &\leq \int g(x) \log(k(x)) dx + \int_{x_0 - \delta}^{x_0 + \delta} g(x) \log\left(1 + \frac{\epsilon}{g(x)}\right) dx \end{aligned}$$

To bound the first integral, note that $\frac{k(x)}{1 - 2\delta\epsilon}$ is a density function, so

$$\begin{aligned} \int g(x) \log(k(x)) dx &= \int g(x) \left(\log\left(\frac{k(x)}{1 - 2\delta\epsilon}\right) + \log(1 - 2\delta\epsilon) \right) dx \\ &\leq \int g(x) (\log(g(x))) dx + \log(1 - 2\delta\epsilon) \end{aligned}$$

Thus

$$\begin{aligned} \int g(x) \log(h(x)) dx &\leq \int g(x) \log(g(x)) dx + \log(1 - 2\delta\epsilon) + \int_{x_0 - \delta}^{x_0 + \delta} g(x) \log\left(1 + \frac{\epsilon}{g(x)}\right) dx \\ &\leq \int g(x) \log(g(x)) dx + \log(1 - 2\delta\epsilon) + 2\delta\epsilon \\ &\leq \int g(x) \log(g(x)) dx - 2\delta^2\epsilon^2 \end{aligned}$$

□

Lemma 1.9. *If g and h are density functions and $h(x) < g(x) - \epsilon$ for all $x \in [x_0 - \delta, x_0 + \delta]$, then the Kulback-Leibler divergence is bounded below by $\int g(x) \log\left(\frac{g(x)}{h(x)}\right) dx > 2\delta^2\epsilon^2 - \frac{8}{3}\delta^3\epsilon^3$*

Proof. Let $h(x) = k(x) - l(x)$, where

$$l(x) = \begin{cases} \epsilon & \text{if } |x - x_0| < \delta \\ 0 & \text{otherwise} \end{cases}$$

Since $h(x) < g(x) - \epsilon$ for all $x \in [x_0 - \delta, x_0 + \delta]$, it follows that $k(x) < g(x)$ for all $x \in [x_0 - \delta, x_0 + \delta]$.

Now $\log(h(x)) = \log(k(x)) + \log\left(1 - \frac{l(x)}{k(x)}\right)$, so

$$\begin{aligned} \int g(x) \log(h(x)) dx &= \int g(x) \log(k(x)) dx + \int_{x_0 - \delta}^{x_0 + \delta} g(x) \log\left(1 - \frac{\epsilon}{k(x)}\right) dx \\ &\leq \int g(x) \log(k(x)) dx + \int_{x_0 - \delta}^{x_0 + \delta} g(x) \log\left(1 - \frac{\epsilon}{g(x)}\right) dx \end{aligned}$$

To bound the first integral, note that $\frac{k(x)}{1+2\delta\epsilon}$ is a density function, so

$$\begin{aligned}\int g(x) \log(k(x)) dx &= \int g(x) \left(\log\left(\frac{k(x)}{1+2\delta\epsilon}\right) + \log(1+2\delta\epsilon) \right) dx \\ &\leq \int g(x) (\log(g(x)) dx + \log(1+2\delta\epsilon))\end{aligned}$$

Thus

$$\begin{aligned}\int g(x) \log(h(x)) dx &\leq \int g(x) \log(g(x)) dx + \log(1+2\delta\epsilon) + \int_{x_0-\delta}^{x_0+\delta} g(x) \log\left(1 - \frac{\epsilon}{g(x)}\right) dx \\ &\leq \int g(x) \log(g(x)) dx + \log(1+2\delta\epsilon) - 2\delta\epsilon \\ &\leq \int g(x) \log(g(x)) dx - 2\delta^2\epsilon^2 + \frac{8}{3}\delta^3\epsilon^3\end{aligned}$$

□

Corollary 1.10. *If density functions g^1 and g are both Lipschitz with constant L , and $\|g^1 - g\|_\infty > \rho$, where $\rho < \sqrt{2L}$, then the Kulback-Leibler divergence is bounded below by $\int g(x) \log\left(\frac{g(x)}{g^1(x)}\right) dx > \frac{\rho^4}{48L^2}$*

Proof. Since $\|g^1 - g\|_\infty > \rho$, there is some x_0 such that $|g^1(x_0) - g(x_0)| > \rho$. By the Lipschitz condition, if we let $\delta = \frac{\rho}{4L}$, then for $x \in [x_0 - \delta, x_0 + \delta]$, we have

$$\begin{aligned}\rho < |(g^1(x_0) - g(x_0))| &= |(g^1(x_0) - g^1(x)) + g^1(x) - g(x) + (g(x) - g(x_0))| \\ &\leq L|x - x_0| + |g^1(x) - g(x)| + L|x - x_0|\end{aligned}$$

so $|g^1(x) - g(x)| > \rho - 2L\delta = \frac{\rho}{2}$. By Lemma 1.8 and Lemma 1.9, we therefore have

$$\int g(x) \log\left(\frac{g(x)}{g^1(x)}\right) dx > 2\left(\frac{\rho^2}{8L}\right)^2 - \frac{8}{3}\left(\frac{\rho^2}{8L}\right)^3$$

It is easy to see that for $\rho < \sqrt{2L}$, this is bounded below by $\frac{\rho^4}{48L^2}$. □

1.2 Constructing \tilde{g}_n

The function \tilde{g}_n is constructed as a kernel density estimate of g with uniform kernel and bandwidth $\delta_n = \left(\frac{\log(n)}{n}\right)^{\frac{1}{4}} \left(\frac{3}{\psi(g)}\right)^{\frac{1}{5}} 2^{0.9} 5^{-0.3}$. That is

$$\tilde{g}_n(x) = \frac{1}{2n\delta_n} \left| \left\{ i \in \{1, \dots, n\} \mid |x_i - x| < \delta_n \right\} \right| = \frac{1}{2\delta_n} \left(G_n(x + \delta_n) - G_n(x - \delta_n) \right)$$

We want to show that \tilde{g}_n has properties (a) and (b).

Proposition 1.11. *If $\|G_n - G\|_\infty \leq \sqrt{\frac{\log(n)}{n}}$, then $\|\tilde{g}_n - g\|_\infty < C_3 \psi(g)^{\frac{1}{5}} \left(\frac{\log(n)}{n}\right)^{\frac{1}{4}}$ where $C_3 = 2^{0.1} 3^{-0.2} 5^{0.3}$.*

Proof. By Lemma 1.5, g is Lipschitz with constant $L = \frac{5^{\frac{3}{5}} \psi(g)^{\frac{2}{5}}}{3^{\frac{2}{5}} 2^{\frac{4}{5}}}$. Since $\tilde{g}_n(x) = \frac{1}{2\delta_n} (G_n(x + \delta_n) - G_n(x - \delta_n))$, For any x ,

$$\begin{aligned}
|\tilde{g}_n(x) - g(x)| &= \left| \frac{1}{2\delta_n} (G_n(x + \delta_n) - G_n(x - \delta_n)) - g(x) \right| \\
&\leq \left| \frac{1}{2\delta_n} ((G_n(x + \delta_n) - G(x + \delta_n)) - (G_n(x - \delta_n) - G(x - \delta_n))) \right| \\
&\quad + \left| \frac{1}{2\delta_n} ((G(x + \delta_n)) - G(x - \delta_n)) - g(x) \right| \\
&\leq \frac{\|G_n - G\|_\infty}{\delta_n} + \left| \frac{1}{2\delta_n} \int_{-\delta_n}^{\delta_n} g(x+t) dt - g(x) \right| \\
&\leq \frac{1}{\delta_n} \sqrt{\frac{\log(n)}{n}} + \left| \frac{1}{2\delta_n} \int_{-\delta_n}^{\delta_n} (g(x+t) - g(x)) dt \right| \\
&\leq \frac{1}{\delta_n} \sqrt{\frac{\log(n)}{n}} + \frac{1}{2\delta_n} \int_{-\delta_n}^{\delta_n} L|t| dt \\
&= \frac{1}{\delta_n} \sqrt{\frac{\log(n)}{n}} + \frac{L\delta_n}{2}
\end{aligned}$$

In particular, since $\delta_n = \left(\frac{\log(n)}{n}\right)^{\frac{1}{4}} \left(\frac{3}{\psi(g)}\right)^{\frac{1}{5}} 2^{0.9} 5^{-0.3}$, we get

$$|\tilde{g}_n(x) - g(x)| \leq 2^{0.1} 5^{0.3} 3^{-0.2} \psi(g)^{0.2} \left(\frac{\log(n)}{n}\right)^{\frac{1}{4}}$$

□

Proposition 1.12. *If $\|G_n - G\|_\infty \leq \sqrt{\frac{\log(n)}{n}}$, then for any function g_L^* that is Lipschitz with constant L , has support S_n , and has $g_L^*(x_i) \geq \epsilon > 0$,*

$$\frac{1}{n} \sum_{i=1}^n \log(g_L^*(x_i)) - \int_{S_n} \tilde{g}_n(x) \log(g_L^*(x)) dx < C_3^{-1} \psi(g)^{-0.2} \left(\frac{\log(n)}{n}\right)^{\frac{1}{4}} \epsilon^{-1} L$$

Proof. We have

$$\begin{aligned}
& \frac{1}{n} \sum_{i=1}^n \log(g_L^*(x_i)) - \int_{S_n} \tilde{g}_n(x) \log(g_L^*(x)) dx \\
&= \frac{1}{n} \sum_{i=1}^n \log(g_L^*(x_i)) - \frac{1}{2\delta_n} \int_{S_n} \left(\frac{1}{n} \sum_{i=1}^n 1_{\{|x_i-x|<\delta_n\}} \right) \log(g_L^*(x)) dx \\
&= \frac{1}{n} \sum_{i=1}^n \frac{1}{2\delta_n} \int_{x_i-\delta_n}^{x_i+\delta_n} (\log(g_L^*(x_i)) - \log(g_L^*(x))) dx \\
&\leq \frac{1}{n} \sum_{i=1}^n \frac{1}{2\delta_n} \int_{x_i-\delta_n}^{x_i+\delta_n} \log \left(1 + \frac{L|x-x_i|}{g_L^*(x)} \right) dx \\
&\leq \frac{1}{n} \sum_{i=1}^n \frac{1}{2\delta_n} \int_{x_i-\delta_n}^{x_i+\delta_n} \frac{L|x-x_i|}{g_L^*(x)} dx \\
&\leq \frac{\delta_n L}{2\epsilon}
\end{aligned}$$

□

1.3 Constructing f_n^*

Controlling the P-MLE is based on finding a lower bound for the penalised maximum likelihood. We do this by exhibiting a good candidate density function that gives high penalised likelihood. A first attempt is the true density function f . However, f can have low likelihood because of a small number of outliers with very low likelihood. To correct for this, we will take a mixture of the true likelihood f and a data-driven likelihood f_n^\dagger that guarantees $g_n^\dagger(x_i) > \epsilon_n$ for $i = 1, \dots, n$.

The easiest way to get an estimator with likelihood bounded below on observed data points is with a kernel density estimate. Since we are trying to find a deconvolved density estimator, this approach does not work — there is no guarantee that the kernel density estimator arises as a convolution with the error distribution. However, by Lemma 1.6, there is a basepoint b for the error distribution, and an $\epsilon > 0$, such that for all $\delta < c$, $P(|E - b| < \delta) > \delta\epsilon$. We let f^\dagger be a kernel estimate from $x_i - b$. Using the condition from Lemma 1.6, we get that if there is an interval about x_0 such that $f^\dagger(x) > a$ for all $x \in [x_0 - \delta, x_0 + \delta]$, then $g^\dagger(x_0 + b) > \epsilon\delta a$.

We want to control the smoothness penalty $\psi(f^\dagger)$. To do this, we set the kernel

$$k_\delta(x) = \delta^{-4} \begin{cases} 3\delta(x+\delta)^2 - 2(x+\delta)^3 & \text{if } -\delta < x \leq 0 \\ 3\delta(x-\delta)^2 + 2(x-\delta)^3 & \text{if } 0 < x < \delta \\ 0 & \text{otherwise} \end{cases}$$

It is easy to check that this kernel has the following properties:

Lemma 1.13. (i) $\int_{-\infty}^{\infty} k_\delta(x) dx = 1$.

(ii) $\psi(k_\delta) = 24\delta^{-5}$

(iii) $k_\delta(0) = \delta^{-1}$

Proof. (i) By symmetry, the positive and negative parts of k_δ have the same integral, so

$$\begin{aligned}
\int_{-\infty}^{\infty} k_\delta(x) dx &= 2\delta^{-4} \int_{-\delta}^0 (3\delta(x+\delta)^2 - 2(x+\delta)^3) dx \\
&= 2\delta^{-4} \int_0^\delta (3\delta t^2 - 2t^3) dt \\
&= 2\delta^{-4} \left[\delta t^3 - \frac{1}{2} t^4 \right]_0^\delta \\
&= 2\delta^{-4} \left(\delta^4 - \frac{1}{2} \delta^4 \right) \\
&= 1
\end{aligned}$$

(ii) We have

$$k_\delta''(x) = \delta^{-4} \begin{cases} 6\delta - 12(x+\delta) & \text{if } -\delta < x \leq 0 \\ 6\delta + 12(x-\delta) & \text{if } 0 < x < \delta \\ 0 & \text{otherwise} \end{cases}$$

so

$$\begin{aligned}
\psi(k_\delta) &= \int_{-\infty}^{\infty} (k_\delta''(x))^2 dx \\
&= \delta^{-8} \int_{-\delta}^\delta (6\delta - 12|x|)^2 dx \\
&= 36\delta^{-8} \int_{-\delta}^\delta (\delta^2 - 4\delta|x| + 4x^2) dx \\
&= 36\delta^{-8} \left(2\delta^3 - 4\delta^3 + \frac{8}{3}\delta^3 \right) \\
&= 24\delta^{-5}
\end{aligned}$$

(iii) This is immediate by evaluating $k_\delta(0)$. □

We can now define $f_n^\dagger(x) = \frac{1}{n} \sum_{i=1}^n k_{\delta_n}(x - x_i + b)$ for some suitably chosen δ_n . We obtain the following properties of f^\dagger for sufficiently large n .

Lemma 1.14. *If $\|G_n - G\|_\infty \leq \sqrt{\frac{\log(n)}{n}}$, and n is sufficiently large, then*

(i) $\int_{-\infty}^{\infty} f^\dagger(x) dx = 1$.

(ii) $\psi(f^\dagger) \leq 48 \left(\frac{5^4 \psi(g)}{12} \right)^{\frac{1}{5}} \delta^{-4}$

(iii) For all $i = 1, \dots, n$, $g^\dagger(x_i) \geq \frac{\epsilon}{4n}$

Proof. (i) This is obvious, since f^\dagger is a mixture of k_δ .

(ii)

$$\begin{aligned}
\psi(f^\dagger) &= \langle f^{\dagger''}, f^{\dagger''} \rangle \\
&= \left\langle \frac{1}{n} \sum k''_{\delta, x_i - b}, \frac{1}{n} \sum k''_{\delta, x_i - b} \right\rangle \\
&= \frac{1}{n^2} \sum_{i=1}^n \sum_{j=1}^n \langle k''_{\delta, x_i - b}, k''_{\delta, x_j - b} \rangle
\end{aligned}$$

For all i, j , $\langle k''_{\delta, x_i - b}, k''_{\delta, x_j - b} \rangle \leq \psi(k_\delta) = 24\delta^{-5}$. On the other hand, if $|x_i - x_j| \geq 2\delta$, then $k''_{\delta, x_i - b}$ and $k''_{\delta, x_j - b}$ have disjoint supports, so $\langle k''_{\delta, x_i - b}, k''_{\delta, x_j - b} \rangle = 0$. Thus

$$\begin{aligned}
\psi(f^\dagger) &\leq \frac{24}{n^2 \delta^5} |\{(i, j) \mid |x_i - x_j| < 2\delta\}| \\
&= \frac{24}{n \delta^5} \sum_{i=1}^n (G_n(x_i + 2\delta) - G_n(x_i - 2\delta)) \\
&\leq \frac{24}{n \delta^5} \sum_{i=1}^n (G(x_i + 2\delta) - G(x_i - 2\delta)) + 2\|G_n - G\|_\infty \\
&\leq \frac{24}{n \delta^5} \sum_{i=1}^n (4\delta\|g\|_\infty + 2\|G_n - G\|_\infty) \\
&\leq \frac{24}{n \delta^5} \sum_{i=1}^n \left(\delta \left(\frac{5^4 \psi(g)}{12} \right)^{\frac{1}{5}} + 2\sqrt{\frac{\log(n)}{n}} \right)
\end{aligned}$$

For large enough n , $2\sqrt{\frac{\log(n)}{n}} \leq \left(\frac{5^4 \psi(g)}{12} \right)^{\frac{1}{5}} \delta$, so $\psi(f^\dagger) \leq 48 \left(\frac{5^4 \psi(g)}{12} \right)^{\frac{1}{5}} \delta^{-4}$

(iii) For $x \in [x_i - b - \frac{\delta}{2}, x_i - b + \frac{\delta}{2}]$, we have $f^\dagger(x) \geq \frac{1}{n} k_\delta(x - (x_i - b)) \geq \frac{1}{n} k_\delta(\frac{\delta}{2}) = \frac{\delta^{-1}}{2n}$. Therefore $g^\dagger(x_i) \geq \epsilon \frac{\delta}{2} \frac{\delta^{-1}}{2n} = \frac{\epsilon}{4n}$. □

Now we define $f_n^*(x) = (1 - \gamma_n)f(x) + \gamma_n f_n^\dagger(x)$, where

$$\gamma_n = \frac{2M\sqrt{\log(n)}}{\sqrt{n} + 2M\sqrt{\log(n)}} \quad (1)$$

and δ_n is the solution to

$$\gamma_n = \left(\sqrt{2} - 1 \right) \delta_n^2 \sqrt{\frac{\psi(f)}{48 \left(\frac{5^4 \psi(g)}{12} \right)^{\frac{1}{5}}}} \quad (2)$$

Proposition 1.15. *For the above definition of $f_n^*(x)$, if $\|G_n - G\|_\infty < \sqrt{\frac{\log(n)}{n}}$ and n is sufficiently large, we have*

(i) $\psi(f_n^*) \leq 2\psi(f)$.

(ii) For $i = 1, \dots, n$, $g_n^*(x_i) \geq (1 - \gamma_n)(g(x_i) \vee r_n)$, where

$$r_n = \frac{\epsilon \gamma_n}{4n} \quad (3)$$

Proof. (i)

$$\psi(f_n^*) \leq (1 - \gamma_n)^2 \psi(f) + 2\gamma_n(1 - \gamma_n) \sqrt{\psi(f)\psi(f^\dagger)} + \gamma_n^2 \psi(f^\dagger) \leq \left(\gamma_n \sqrt{\psi(f^\dagger)} + \sqrt{\psi(f)} \right)^2$$

Substituting $\gamma_n = (\sqrt{2} - 1) \delta_n^2 \sqrt{\frac{\psi(f)}{48 \left(\frac{5^4 \psi(g)}{12} \right)^{\frac{1}{5}}}}$ and $\psi(f^\dagger) \leq 48 \left(\frac{5^4 \psi(g)}{12} \right)^{\frac{1}{5}} \delta^{-4}$ (from Lemma 1.14)

gives

$$\gamma_n \sqrt{\psi(f^\dagger)} \leq (\sqrt{2} - 1) \sqrt{\psi(f)}$$

so $\psi(f_n^*) < 2\psi(f)$.

(ii)

$$\begin{aligned} g_n^*(x_i) &= \gamma_n g^\dagger(x_i) + (1 - \gamma_n)g(x_i) \\ &\geq \frac{\gamma_n \epsilon}{4n} \vee (1 - \gamma_n)g(x_i) \\ &= (1 - \gamma_n) \left(g(x_i) \vee \frac{\gamma_n \epsilon}{4n(1 - \gamma_n)} \right) \\ &\geq (1 - \gamma_n) \left(g(x_i) \vee \frac{\gamma_n \epsilon}{4n} \right) \end{aligned}$$

□

This means that

$$\frac{1}{n} \sum_{i=1}^n \log(g_n^*(x_i)) \geq \log(1 - \gamma_n) + \frac{1}{n} \sum_{i=1}^n \log(b(x_i))$$

where $b_n(x) = g(x) \vee r_n$ where $r_n = \frac{\gamma_n \epsilon}{4n}$.

Proposition 1.16. *Whenever, $\|G_n - G\| < \sqrt{\frac{\log(n)}{n}}$, and n is sufficiently large*

$$\frac{1}{n} \sum_{i=1}^n \log(g_n^*(x_i)) > -H(g) - 3M \log(n)^{\frac{3}{2}} n^{-\frac{1}{2}}$$

where $H(g)$ is the entropy $-\int_{-\infty}^{\infty} g(x) \log(g(x))$

Proof. We set $b_n(x) = g(x) \vee r_n$, so that for all $i = 1, \dots, n$, $g_n^*(x_i) \geq (1 - \gamma_n)b_n(x_i)$.

$$\begin{aligned}
\frac{1}{n} \sum_{i=1}^n \log(b_n(x_i)) &= \log(r_n) - \int_{-\infty}^{\infty} G_n(x) \left(\frac{d}{dx} \log(b_n(x)) \right) dx \\
&= \log(r_n) - \int_{-\infty}^{\infty} G_n(x) \left(\frac{b'_n(x)}{b_n(x)} \right) dx \\
&= \log(r_n) - \int_{-\infty}^{\infty} G(x) \left(\frac{b'_n(x)}{b_n(x)} \right) dx + \int_{-\infty}^{\infty} (G(x) - G_n(x)) \left(\frac{b'_n(x)}{b_n(x)} \right) dx \\
&= \int_{-\infty}^{\infty} g(x) \log(b_n(x)) dx + \int_{-\infty}^{\infty} (G(x) - G_n(x)) \left(\frac{b'_n(x)}{b_n(x)} \right) dx \\
&\geq -H(g) - \|G(x) - G_n(x)\|_{\infty} \int_{-\infty}^{\infty} \left| \frac{b'_n(x)}{b_n(x)} \right| dx \\
\frac{1}{n} \sum_{i=1}^n \log(g_n^*(x_i)) &\geq -H(g) + \log(1 - \gamma_n) - \|G(x) - G_n(x)\|_{\infty} \frac{2M}{5} \log \left(\frac{5^4 \psi(g)}{3 \times 2^{12} r_n^5} \right) \\
&\geq -H(g) + \log(1 - \gamma_n) - \frac{2M}{5} \log \left(\frac{5^4 \psi(g)}{3 \times 2^{12} r_n^5} \right) \sqrt{\frac{\log(n)}{n}}
\end{aligned}$$

where the last line is by Proposition 1.7. Substituting $\gamma_n = \frac{c_n}{1+c_n}$ where $c_n = 2M\sqrt{\frac{\log(n)}{n}}$, and letting $K_n = \left(\frac{5^4 \psi(g)}{3 \times 2^{12}} \right)^{\frac{1}{5}} r_n^{-1}$, this inequality becomes

$$\frac{1}{n} \sum_{i=1}^n \log(g_n^*(x_i)) \geq -H(g) - c_n \log(K_n) - \log(c_n + 1)$$

We have $\log(c_n + 1) \leq c_n$, and for large enough n , we have $n^3 > e^2 K_n^2$, so $\log(K_n) + 1 < \frac{3 \log(n)}{2}$. Thus, the inequality becomes

$$\frac{1}{n} \sum_{i=1}^n \log(g_n^*(x_i)) \geq -H(g) - \frac{3c_n \log(n)}{2}$$

□

1.4 Proving Consistency

In this section, we use the \tilde{g}_n and f_n^* defined in the previous sections to show that provided $\frac{|S_n| \log(n)^{\frac{1}{4}}}{n^{\frac{1}{4}}} \rightarrow 0$, when we set $\lambda_n = C_1 n^{\frac{7}{8}} \log(n)^{\frac{1}{8}} \sqrt{|S_n|}$, where $C_1 = \frac{2^{\frac{31}{20}} 3^{-\frac{1}{10}} 5^{\frac{3}{20}}}{\psi(f_x)^{\frac{1}{5}} \psi(g)^{\frac{1}{10}}}$, our method is consistent.

Lemma 1.17. *If g and h are density functions with support S , and $a > 0$ then $\int_S g(x) \log(h(x) \vee a) dx \leq -H(g) + a|S|$.*

Proof.

$$\begin{aligned}
\int_S g(x) \log(h(x) \vee a) dx + H(g) &= \int_S g(x) \log\left(\frac{h(x) \vee a}{g(x)}\right) dx \\
&\leq \int_S g(x) \left(\frac{h(x) \vee a - g(x)}{g(x)}\right) dx \\
&\leq \int_S (h(x) + a - g(x)) dx \\
&= 1 + a|S| - 1 = a|S|
\end{aligned}$$

□

Proposition 1.18. *If $\|G_n - G\| \leq \sqrt{\frac{\log(n)}{n}}$, and n is sufficiently large, then $\psi(\hat{f}_n) \leq 3\psi(f)$.*

Proof. By Propositions 1.16 and 1.15(i), the penalised likelihood of f_n^* is at least

$$-n \left(H(g) + 3M \log(n)^{\frac{3}{2}} n^{-\frac{1}{2}} \right) - 2\lambda_n \psi(f)$$

Since \hat{f}_n maximises the penalised likelihood, we have that

$$\sum_{i=1}^n \log(\hat{g}_n(x_i)) - \lambda_n \psi(\hat{f}_n) \geq -n \left(H(g) + 3M \log(n)^{\frac{3}{2}} n^{-\frac{1}{2}} \right) - 2\lambda_n \psi(f) \quad (4)$$

By Lemmas 1.2 and 1.5, \hat{g}_n is Lipschitz with constant $L = \left(\frac{125}{144}\right)^{\frac{1}{5}} \psi(\hat{f}_n)^{\frac{2}{5}}$. By Proposition 1.12, we have that for any $0 < a < 1$,

$$\begin{aligned}
\sum_{i=1}^n \log(\hat{g}_n(x_i)) &\leq \sum_{i=1}^n \log(\hat{g}_n(x_i) \vee a) \\
&\leq n \int_{S_n} \tilde{g}_n(x) \log(\hat{g}_n(x) \vee a) dx + \frac{n^{\frac{3}{4}} \log(n)^{\frac{1}{4}} L}{C_3 \psi(g)^{\frac{1}{5}} a}
\end{aligned} \quad (5)$$

Meanwhile, we have

$$\begin{aligned}
\int_{S_n} \tilde{g}_n(x) \log(\hat{g}_n(x) \vee a) dx &= \int_{S_n} (g(x) + \tilde{g}_n(x) - g(x)) \log(\hat{g}_n(x) \vee a) dx \\
&\leq \int_{S_n} g(x) \log(\hat{g}_n(x) \vee a) dx + |S_n| \|\tilde{g}_n - g\|_{\infty} \sup(|\log(\hat{g}_n(x) \vee a)|) \\
&\leq -H(g) + a|S_n| + |S_n| \|\tilde{g}_n - g\|_{\infty} (\log(\sup(\hat{g}_n(x))) \vee (-\log(a)))
\end{aligned}$$

Since \hat{g}_n is Lipschitz with constant L , the equation $\int_{-\infty}^{\infty} \hat{g}_n(x) dx = 1$ gives $\sup \hat{g}_n(x) \leq \sqrt{L}$, and by Proposition 1.11, $\|\tilde{g}_n - g\|_{\infty} \leq C_3 \psi(g)^{\frac{1}{5}} \left(\frac{\log(n)}{n}\right)^{\frac{1}{4}}$ so

$$\log(\sup(\hat{g}_n(x))) \vee (-\log(a)) \leq \log\left(\sqrt{L} \vee a^{-1}\right) = \frac{1}{2} \log(L \vee a^{-2})$$

Therefore,

$$\int_{S_n} \tilde{g}_n(x) \log(\hat{g}_n(x) \vee a) dx \leq -H(g) + a|S_n| + \frac{C_3}{2} \psi(g)^{\frac{1}{5}} |S_n| \left(\frac{\log(n)}{n}\right)^{\frac{1}{4}} \log(L \vee a^{-2})$$

Substituting this into (5), and substituting the result into (4) gives

$$\begin{aligned}
-n \left(H(g) + 3Mn^{-\frac{1}{2}} \log(n)^{\frac{3}{2}} \right) - 2\lambda_n \psi(f) &\leq n \left(-H(g) + a|S_n| + \frac{C_3}{2} \psi(g)^{\frac{1}{5}} |S_n| \left(\frac{\log(n)}{n} \right)^{\frac{1}{4}} \log(L \vee a^{-2}) \right) \\
&\quad + \frac{n^{\frac{3}{4}} \log(n)^{\frac{1}{4}}}{C_3 \psi(g)^{\frac{1}{5}} a} L - \lambda_n \psi(\hat{f}_n) \\
-3Mn^{\frac{1}{2}} \log(n)^{\frac{3}{2}} - 2\lambda_n \psi(f) &\leq \frac{n}{2} |S_n| \left(2a + C_3 \psi(g)^{\frac{1}{5}} \left(\frac{\log(n)}{n} \right)^{\frac{1}{4}} (\log(L \vee a^{-2})) \right) \\
&\quad + \frac{n^{\frac{3}{4}} \log(n)^{\frac{1}{4}}}{C_3 \psi(g)^{\frac{1}{5}} a} L - \lambda_n \psi(\hat{f}_n)
\end{aligned} \tag{6}$$

Since a is arbitrary here, we can set $a = \left(\frac{\log(n)}{n} \right)^{\frac{1}{8}} \frac{\sqrt{L}}{\psi(g)^{\frac{1}{10}} \sqrt{C_3 |S_n|}}$ so that $an|S_n| + \frac{n^{\frac{3}{4}} \log(n)^{\frac{1}{4}}}{C_3 \psi(g)^{\frac{1}{5}} a} L = C_4 n^{\frac{7}{8}} \log(n)^{\frac{1}{8}} \sqrt{L} \sqrt{|S_n|}$, where $C_4 = 2\psi(g)^{-\frac{1}{10}} C_3^{-\frac{1}{2}}$. Also, if $\psi(\hat{f}_n) \leq 3\psi(f)$, then the proposition is true. Otherwise, $a^{-2} = \frac{n^{\frac{1}{4}} \psi(g)^{\frac{1}{5}} C_3 |S_n|}{L \log(n)^{\frac{1}{4}}} \leq \frac{n^{\frac{1}{4}} \psi(g)^{\frac{1}{5}} C_3 |S_n|}{\left(\frac{125}{144} \right)^{\frac{1}{5}} (3\psi(f))^{\frac{2}{5}} \log(n)^{\frac{1}{4}}}$. For large enough n , we have $a^{-2} > L$, so we rearrange (6) to get

$$\begin{aligned}
&\psi(\hat{f}_n) - 2\psi(f) \\
\leq \frac{1}{\lambda_n} &\left(\frac{C_3 \psi(g)^{\frac{1}{5}}}{2} n^{\frac{3}{4}} |S_n| \log(n)^{\frac{1}{4}} \left(\log \left(\frac{C_3 \psi(g)^{\frac{1}{5}} |S_n| n^{\frac{1}{4}}}{\left(\frac{125}{16} \right)^{\frac{1}{5}} \psi(f)^{\frac{1}{5}} \log(n)^{\frac{1}{4}}} \right) \right) + 3Mn^{\frac{1}{2}} \log(n)^{\frac{3}{2}} + C_4 n^{\frac{7}{8}} \log(n)^{\frac{1}{8}} \sqrt{L} \sqrt{|S_n|} \right)
\end{aligned}$$

Substituting $L = \left(\frac{125}{144} \right)^{\frac{1}{5}} \psi(\hat{f}_n)^{\frac{2}{5}}$ and rearranging gives

$$\psi(\hat{f}_n) - \alpha_n \psi(\hat{f}_n)^{\frac{1}{5}} \leq \beta_n + 2\psi(f)$$

where

$$\begin{aligned}
\alpha_n &= \frac{C_4 n^{\frac{7}{8}} \log(n)^{\frac{1}{8}} \sqrt{|S_n|}}{\lambda_n} \left(\frac{125}{144} \right)^{\frac{1}{10}} \\
\beta_n &= \frac{C_3 \psi(g)^{\frac{1}{5}}}{2\lambda_n} n^{\frac{3}{4}} |S_n| \log(n)^{\frac{1}{4}} \log \left(\frac{C_3 \psi(g)^{\frac{1}{5}} |S_n| n^{\frac{1}{4}}}{\left(\frac{125}{16} \right)^{\frac{1}{5}} \psi(f)^{\frac{1}{5}} \log(n)^{\frac{1}{4}}} \right) + \frac{3Mn^{\frac{1}{2}} \log(n)^{\frac{3}{2}}}{\lambda_n}
\end{aligned}$$

We have defined λ_n to satisfy $\lambda_n = \frac{2C_4}{\psi(f)^{\frac{1}{5}}} n^{\frac{7}{8}} \log(n)^{\frac{1}{8}} \sqrt{|S_n|} \left(\frac{125}{144} \right)^{\frac{1}{10}}$, so that $\alpha_n = \frac{\psi(f)^{\frac{1}{5}}}{2}$ and $\beta_n \rightarrow 0$, so for large enough n , $\beta_n < \left(1 - \frac{1}{2} \times 3^{\frac{1}{5}} \right) \psi(f)$, so we have $\frac{\psi(\hat{f}_n)}{\psi(f)} - \frac{1}{2} \left(\frac{\psi(\hat{f}_n)}{\psi(f)} \right)^{\frac{1}{5}} < 3 - \frac{1}{2} \times 3^{\frac{1}{5}}$, which gives $\psi(\hat{f}_n) < 3\psi(f)$. \square

This proves that \hat{f}_n is Lipschitz. Under this Lipschitz condition, we can show that if \hat{g}_n is too far from g , then its penalised likelihood will be less than the penalised likelihood of g_n^* , contradicting the maximality.

Proposition 1.19. *If $\|g_L - g\|_{\infty} \geq \rho_n$, where g and g_L are both Lipschitz density functions with constant L , and $\|G_n - G\|_{\infty} < \sqrt{\frac{\log(n)}{n}}$, then*

$$\frac{1}{n} \sum_{i=1}^n \log(g_L(x_i)) \leq -H(g) - \frac{\rho_n^4}{1536L^2} + \left(\frac{\log(n)}{n}\right)^{\frac{1}{4}} |S_n| \left(\frac{1536L^3}{C_3\psi(g)^{\frac{1}{5}}\rho_n^4} + C_3\psi(g)^{\frac{1}{5}} \log\left(\frac{1536|S_n|L^{\frac{5}{2}}}{\rho_n^4}\right) \right)$$

Proof. By Proposition 1.12, we have that for any $a > 0$,

$$\begin{aligned} \frac{1}{n} \sum_{i=1}^n \log(g_L(x_i)) &\leq \frac{1}{n} \sum_{i=1}^n \log(g_L(x_i) \vee a) \\ &\leq \int_{S_n} \tilde{g}_n(x) \log(g_L(x) \vee a) dx + \frac{\log(n)^{\frac{1}{4}} L}{C_3\psi(g)^{\frac{1}{5}} n^{\frac{1}{4}} a} \end{aligned}$$

We use Proposition 1.11 to show

$$\begin{aligned} \int_{S_n} \tilde{g}_n(x) \log(g_L(x) \vee a) dx &= \int_{S_n} (g(x) + \tilde{g}_n(x) - g(x)) \log(g_L(x) \vee a) dx \\ &\leq \int_{S_n} g(x) \log(g_L(x) \vee a) dx + |S_n| \|\tilde{g}_n - g\|_{\infty} \log\left(\frac{\sup_{x \in S_n} (g_L(x) \vee 1)}{a}\right) \\ &\leq \int_{S_n} g(x) \log(g_L(x) \vee a) dx \\ &\quad + C_3\psi(g)^{\frac{1}{5}} \left(\frac{\log(n)}{n}\right)^{\frac{1}{4}} |S_n| \log\left(\frac{\sup_{x \in S_n} (g_L(x) \vee 1)}{a}\right) \end{aligned}$$

Let $\int_{S_n} g_L(x) \vee a dx = c$. Clearly $1 \leq c \leq 1 + a|S_n|$. Let $b(x) = \frac{g_L(x) \vee a}{c}$. By definition, $b(x)$ is a density function, and is Lipschitz with constant L , and $\|b - g\|_{\infty} \geq \rho_n - ((c-1)\|g_L\|_{\infty} \vee a)$, since for any x ,

$$|b(x) - g_L(x)| = \left| \frac{g_L(x) \vee a}{c} - g_L(x) \right| = \begin{cases} (1 - \frac{1}{c})g_L(x) & \text{if } g_L(x) > a \\ \frac{a}{c} - g_L(x) & \text{if } g_L(x) \leq a \end{cases} \leq (c-1)g_L(x) \vee a$$

Since $\|g_L - g\|_{\infty} \geq \rho_n$, there is some x for which $|g_L(x) - g(x)| \geq \rho_n$. For this x , $|b(x) - g(x)| \geq |g_L(x) - g(x)| - |g_L(x) - b(x)| \geq \rho_n - ((c-1)\|g_L\|_{\infty} \vee a)$. Now by Corollary 1.10,

$$\begin{aligned} \int_{S_n} g(x) \log(g_L(x) \vee a) dx &= \int_{S_n} g(x) \log(cb(x)) dx \\ &= \int_{S_n} g(x)(\log(b(x)) + \log(c)) dx \\ &\leq -H(g) - \frac{(\rho_n - ((c-1)\|g_L\|_{\infty} \vee a)^4}{48L^2} + \log(c) \end{aligned}$$

Thus, using the fact that $(c-1)\|g_L\|_{\infty} \leq a|S_n|\|g_L\|_{\infty}$, and $|S_n|\|g_L\|_{\infty} \geq \int_{S_n} g_L(x) dx = 1$, we get

$$\begin{aligned} \frac{1}{n} \sum_{i=1}^n \log(g_L(x_i)) &\leq -H(g) - \frac{(\rho_n - a(|S_n| \|g_L\|_\infty))^4}{48L^2} + \log(1 + a|S_n|) \\ &\quad + C_3 \psi(g)^{\frac{1}{5}} \left(\frac{\log(n)}{n} \right)^{\frac{1}{4}} |S_n| \log \left(\frac{\sup_{x \in S_n} (g_L(x) \vee 1)}{a} \right) \\ &\quad + \frac{\log(n)^{\frac{1}{4}} L}{C_3 \psi(g)^{\frac{1}{5}} n^{\frac{1}{4}} a} \end{aligned}$$

for any $a > 0$. In particular, we choose $a = \frac{\rho_n^4}{1536L^2|S_n|}$. Since

$$\rho_n \leq \|g_L - g\|_\infty \leq \|g_L\|_\infty + \|g\|_\infty \leq 2\sqrt{L} < 768^{\frac{1}{3}} \sqrt{L} \leq \left(\frac{768L^2}{\|g_L\|_\infty} \right)^{\frac{1}{3}}$$

(because $\|g_L\|_\infty \leq \sqrt{L}$, by the Lipschitz condition), it follows that $a \leq \frac{\rho_n}{2|S_n|\|g_L\|_\infty}$, so we have $\frac{(\rho_n - a|S_n|\|g_L\|_\infty)^4}{48L^2} \geq \frac{\rho_n^4}{768L^2}$ and $\log(1 + a|S_n|) \leq \frac{\rho_n^4}{1536L^2}$, so that

$$\begin{aligned} \frac{1}{n} \sum_{i=1}^n \log(g_L(x_i)) &\leq -H(g) - \frac{\rho_n^4}{1536L^2} + \frac{1536 \log(n)^{\frac{1}{4}} |S_n| L^3}{C_3 \psi(g)^{\frac{1}{5}} n^{\frac{1}{4}} \rho_n^4} \\ &\quad + C_3 \psi(g)^{\frac{1}{5}} \left(\frac{\log(n)}{n} \right)^{\frac{1}{4}} |S_n| \log \left(\frac{1536|S_n|L^2}{\rho_n^4} \left(\sup_{x \in S_n} g_L(x) \vee 1 \right) \right) \end{aligned}$$

By the Lipschitz condition, $\|g_L\|_\infty \leq \sqrt{L}$, so for $L \geq 1$,

$$\frac{1}{n} \sum_{i=1}^n \log(g_L(x_i)) \leq -H(g) - \frac{\rho_n^4}{1536L^2} + \left(\frac{\log(n)}{n} \right)^{\frac{1}{4}} |S_n| \left(\frac{1536L^3}{C_3 \psi(g)^{\frac{1}{5}} \rho_n^4} + C_3 \psi(g)^{\frac{1}{5}} \log \left(\frac{1536|S_n|L^{\frac{5}{2}}}{\rho_n^4} \right) \right)$$

□

This allows us to show

Theorem 1.20. *If $\|G_n - G\|_\infty < \sqrt{\frac{\log(n)}{n}}$ and $\lambda_n = C_1 n^{\frac{7}{8}} \log(n)^{\frac{1}{8}} \sqrt{|S_n|}$, where $C_1 = \frac{2C_4}{\psi(f)^{\frac{1}{5}}} \left(\frac{125}{144} \right)^{\frac{1}{10}} = \frac{2^{\frac{31}{20}} 3^{-\frac{1}{10}} 5^{\frac{3}{20}}}{\psi(f)^{\frac{1}{5}} \psi(g)^{\frac{1}{10}}}$, then for sufficiently large n , $\|\hat{g}_n - g\|_\infty < C_2 n^{-\frac{1}{32}} |S_n|^{\frac{1}{8}} \log(n)^{\frac{1}{32}}$ for some constant C_2 (depending on $\psi(f)$ and $\psi(g)$).*

Proof. By Proposition 1.18 and Lemma 1.5, g and \hat{g}_n are both Lipschitz with constant $L = \left(\frac{125}{16} \right)^{\frac{1}{5}} \times \psi(f)^{\frac{2}{5}}$. Let $\rho_n = \|\hat{g}_n - g\|_\infty$. By Proposition 1.19,

$$\frac{1}{n} \sum_{i=1}^n \log(\hat{g}_n(x_i)) \leq -H(g) - \frac{\rho_n^4}{1536L^2} + \left(\frac{\log(n)}{n} \right)^{\frac{1}{4}} |S_n| \left(\frac{1536L^3}{C_3 \psi(g)^{\frac{1}{5}} \rho_n^4} + C_3 \psi(g)^{\frac{1}{5}} \log \left(\frac{1536|S_n|L^{\frac{5}{2}}}{\rho_n^4} \right) \right)$$

If $\rho_n > n^{-1} \left(1536|S_n|L^{\frac{5}{2}} \right)^{\frac{1}{4}}$, we have $\log \left(\frac{1536|S_n|L^{\frac{5}{2}}}{\rho_n^4} \right) < 4 \log(n)$, so

$$\frac{1}{n} \sum_{i=1}^n \log(\hat{g}_n(x_i)) \leq -H(g) - \frac{\rho_n^4}{1536L^2} + \frac{1536 \log(n)^{\frac{1}{4}} |S_n| L^3}{C_3 \psi(g)^{\frac{1}{5}} n^{\frac{1}{4}} \rho_n^4} + 4C_3 \psi(g)^{\frac{1}{5}} \frac{\log(n)^{\frac{5}{4}}}{n^{\frac{1}{4}}} |S_n|$$

On the other hand, by Proposition 1.16,

$$\frac{1}{n} \sum_{i=1}^n \log(\hat{g}_n(x_i)) - \frac{\lambda_n}{n} \psi(\hat{f}_n) \geq \frac{1}{n} \sum_{i=1}^n \log(g_n^*(x_i)) - \frac{\lambda_n}{n} \psi(f_n^*) \geq -H(g) - 3M \log(n)^{\frac{3}{2}} n^{-\frac{1}{2}} - \frac{2\lambda_n}{n} \psi(f)$$

Thus we have

$$-\frac{\rho_n^4}{1536L^2} + \frac{1536 \log(n)^{\frac{1}{4}} |S_n| L^3}{C_3 \psi(g)^{\frac{1}{5}} n^{\frac{1}{4}} \rho_n^4} + 4C_3 \psi(g)^{\frac{1}{5}} \frac{\log(n)^{\frac{5}{4}}}{n^{\frac{1}{4}}} |S_n| - \frac{\lambda_n}{n} \psi(\hat{f}_n) \geq -3M \log(n)^{\frac{3}{2}} n^{-\frac{1}{2}} - \frac{2\lambda_n}{n} \psi(f)$$

$$\frac{\rho_n^4}{1536L^2} - \frac{1536 \log(n)^{\frac{1}{4}} |S_n| L^3}{C_3 \psi(g)^{\frac{1}{5}} n^{\frac{1}{4}} \rho_n^4} \leq 4C_3 \psi(g)^{\frac{1}{5}} \frac{\log(n)^{\frac{5}{4}}}{n^{\frac{1}{4}}} |S_n| + 3M \log(n)^{\frac{3}{2}} n^{-\frac{1}{2}} + \frac{\lambda_n}{n} (2\psi(f) - \psi(\hat{f}_n))$$

For large enough n , $n^{-\frac{1}{4}} \log(n)^{\frac{1}{4}} |S_n|^{-1} < \frac{C_3 \psi(g)^{\frac{1}{5}}}{3M}$, so

$$\frac{\rho_n^4}{1536L^2} - \frac{1536 \log(n)^{\frac{1}{4}} |S_n| L^3}{C_3 \psi(g)^{\frac{1}{5}} n^{\frac{1}{4}} \rho_n^4} \leq 5C_3 \psi(g)^{\frac{1}{5}} \log(n)^{\frac{5}{4}} n^{-\frac{1}{4}} |S_n| + \frac{\lambda_n}{n} (2\psi(f) - \psi(\hat{f}_n))$$

With

$$\lambda_n = \frac{2C_4}{\psi(f)^{\frac{4}{5}}} n^{\frac{7}{8}} \log(n)^{\frac{1}{8}} \sqrt{|S_n|} \left(\frac{125}{144} \right)^{\frac{1}{10}}$$

for large enough n , and since $\psi(\hat{f}_n) > 0$, we deduce

$$\frac{\lambda_n}{n} (2\psi(f) - \psi(\hat{f}_n)) \leq \frac{2\lambda_n \psi(f)}{n} = 2C_4 \psi(f)^{\frac{1}{5}} n^{-\frac{1}{8}} \log(n)^{\frac{1}{8}} \sqrt{|S_n|} \left(\frac{125}{144} \right)^{\frac{1}{10}}$$

so

$$\frac{\rho_n^4}{1536L^2} - \frac{1536 \log(n)^{\frac{1}{4}} |S_n| L^3}{C_3 \psi(g)^{\frac{1}{5}} n^{\frac{1}{4}} \rho_n^4} \leq 5C_3 \psi(g)^{\frac{1}{5}} \log(n)^{\frac{5}{4}} n^{-\frac{1}{4}} |S_n| + C_5 n^{-\frac{1}{8}} |S_n|^{\frac{1}{2}} \log(n)^{\frac{1}{8}}$$

where $C_5 = 2C_4 \psi(f)^{\frac{1}{5}} \left(\frac{125}{144} \right)^{\frac{1}{10}}$. For sufficiently large n , the first term on the right-hand side is much smaller than the second, so we get

$$\frac{\rho_n^4}{1536L^2} - \frac{1536 \log(n)^{\frac{1}{4}} |S_n| L^3}{C_3 \psi(g)^{\frac{1}{5}} n^{\frac{1}{4}} \rho_n^4} \leq 2C_5 n^{-\frac{1}{8}} |S_n|^{\frac{1}{2}} \log(n)^{\frac{1}{8}}$$

Rewriting this as $a_n(\rho_n)^8 - b_n(\rho_n)^4 - c_n \leq 0$ where

$$\begin{aligned} a_n &= \frac{1}{1536L^2} \\ b_n &= 2C_5 n^{-\frac{1}{8}} |S_n|^{\frac{1}{2}} \log(n)^{\frac{1}{8}} \\ c_n &= \frac{1536 \log(n)^{\frac{1}{4}} |S_n| L^3}{C_3 \psi(g)^{\frac{1}{5}} n^{\frac{1}{4}}} \end{aligned}$$

we deduce

$$\begin{aligned}
(\rho_n)^4 &\leq \frac{b_n + \sqrt{b_n^2 + 4a_n c_n}}{2a_n} \\
&= 768L^2 \left(2C_5 n^{-\frac{1}{8}} |S_n|^{\frac{1}{2}} \log(n)^{\frac{1}{8}} + \sqrt{\left(2C_5 n^{-\frac{1}{8}} |S_n|^{\frac{1}{2}} \log(n)^{\frac{1}{8}} \right)^2 + \frac{4 \log(n)^{\frac{1}{4}} |S_n| L}{C_3 \psi(g)^{\frac{1}{5}} n^{\frac{1}{4}}}} \right) \\
&= 768L^2 n^{-\frac{1}{8}} |S_n|^{\frac{1}{2}} \log(n)^{\frac{1}{8}} \left(2C_5 + \sqrt{4C_5^2 + \frac{4L}{C_3 \psi(g)^{\frac{1}{5}}}} \right)
\end{aligned}$$

Thus

$$\rho_n \leq C_2 \log(n)^{\frac{1}{32}} |S_n|^{\frac{1}{8}} n^{-\frac{1}{32}}$$

where, plugging in all the constants,

$$C_2 = \left(1 + \sqrt{1 + \frac{3^{\frac{2}{5}}}{16}} \right)^{\frac{1}{4}} 2^{\frac{179}{80}} 3^{\frac{9}{40}} 5^{\frac{27}{80}} \psi(f)^{\frac{1}{4}} \psi(g)^{-\frac{1}{40}}$$

□

From this, and the Dvoretzky-Kiefer-Wolfowitz inequality, Theorem 1.1 follows immediately.

2 Additional Simulation Results

Figures S1–S8 show box plots for all simulation scenarios not shown in the main paper. Like the scenarios shown in the main paper, we see that P-MLE is consistently better than the other methods in the vast majority of cases, rather than the differences in MISE being due to a small number of outliers in MISE.

3 Effect of λ_n

For the simulations, we wanted to know how much the results could be improved with a better choice of the smoothness penalty λ_n . We reran the scenarios where P-MLE did not outperform the other methods using different ratios for the heuristic method of setting λ_n . We ran each scenario using values 1000, 10000, 100000, 1000000, and 10000000 for the ratio in the heuristic for setting λ_n . We then looked at the best results in each scenario. In 9 of the scenarios, there was a difference from the outcome reported in Table 8 in the main paper. This is selecting the value of λ_n which performs best on the data, so is not a completely reliable estimate of performance. However, it shows that there is potential to improve performance with a better choice of λ_n . Furthermore, these results are using the same heuristic for λ_n for all simulations in each scenario, rather than tuning the value of λ_n for each simulation. It is therefore possible that more careful tuning could improve the performance of P-MLE still further.

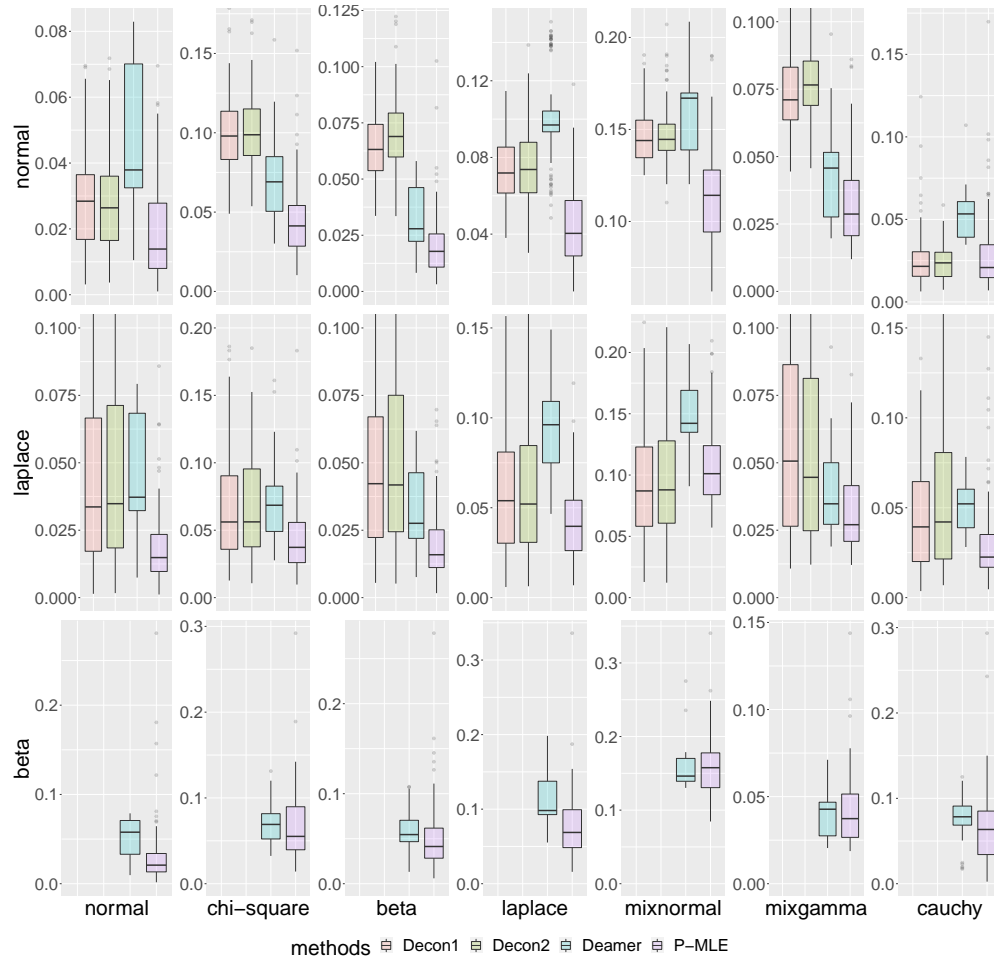


Figure S1: Sample distribution of ISE for sample size 30 and SNR 4. Each column corresponds to one of the seven true distributions in the simulation. Rows correspond to the error distribution. The `decon` package only allows a limited selection of error families, so could not be compared for simulations with a beta error. Some outliers where `decon` produced a large ISE are truncated from these plots. No P-MLE results have been truncated.

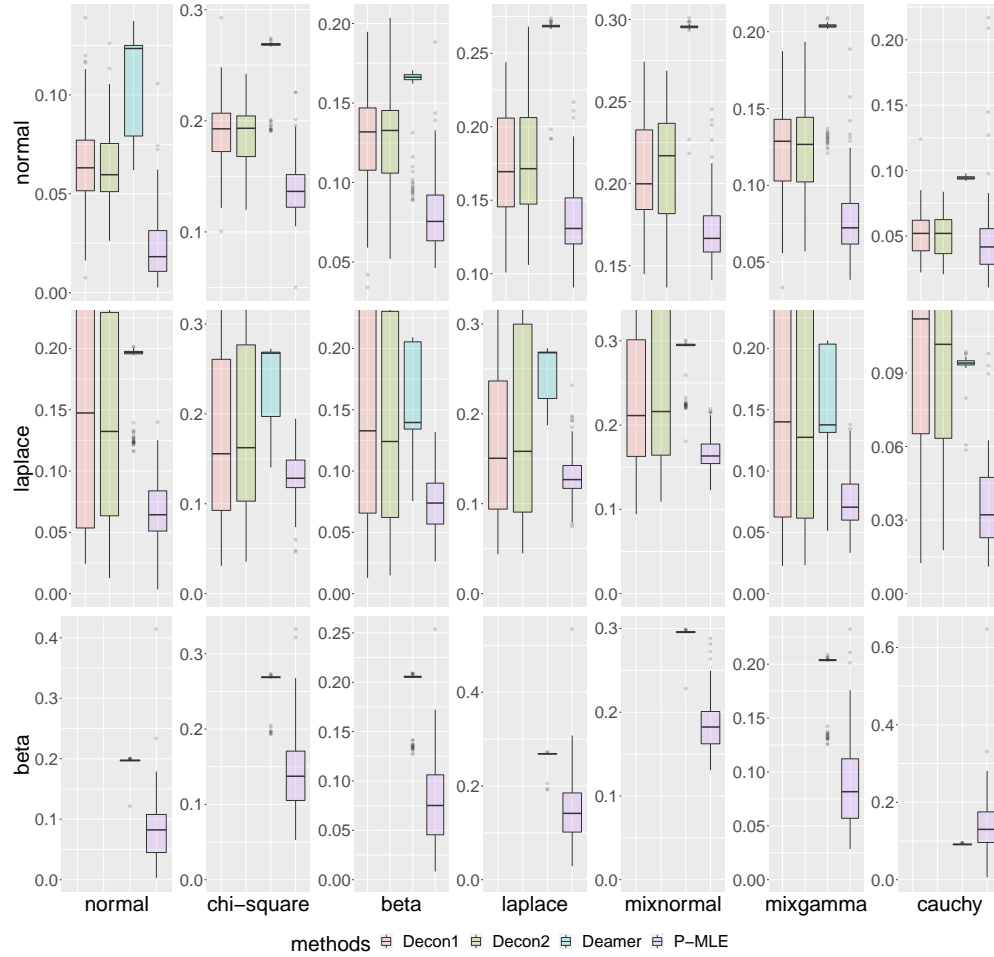


Figure S2: Sample distribution of ISE for sample size 30 and SNR 0.25. Each column corresponds to one of the seven true distributions in the simulation. Rows correspond to the error distribution. The `decon` package only allows a limited selection of error families, so could not be compared for simulations with a beta error. Some outliers where `decon` produced a large ISE are truncated from these plots. No P-MLE results have been truncated.

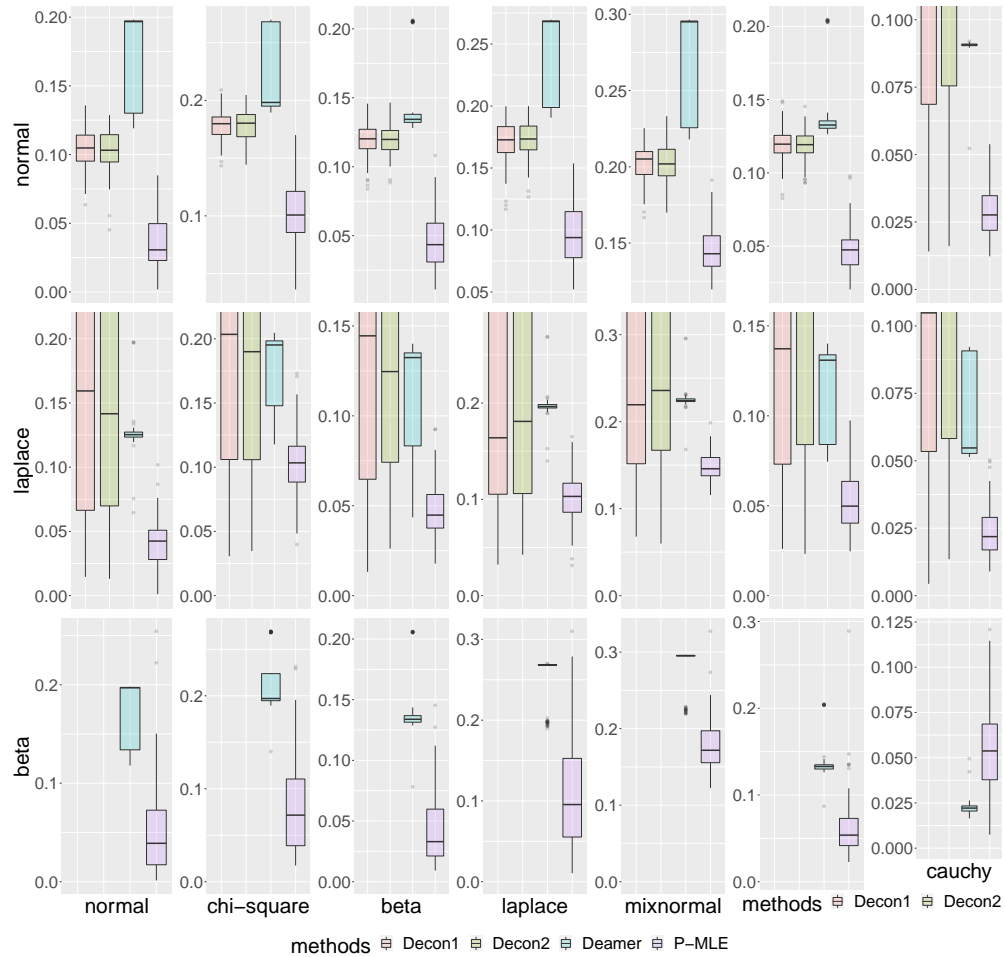


Figure S3: Sample distribution of ISE for sample size 100 and SNR 4. Each column corresponds to one of the seven true distributions in the simulation. Rows correspond to the error distribution. The `decon` package only allows a limited selection of error families, so could not be compared for simulations with a beta error. Some outliers where `decon` produced a large ISE are truncated from these plots. No P-MLE results have been truncated.

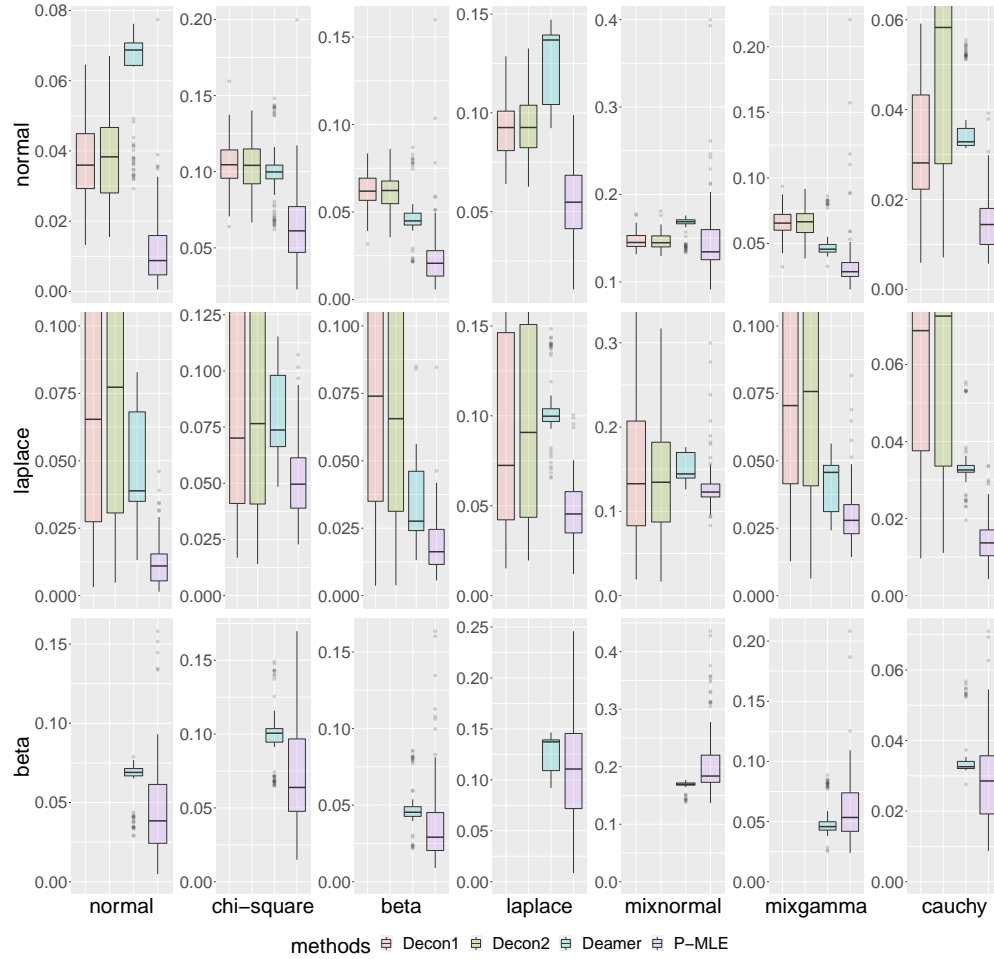


Figure S4: Sample distribution of ISE for sample size 100 and SNR 1. Each column corresponds to one of the seven true distributions in the simulation. Rows correspond to the error distribution. The `decon` package only allows a limited selection of error families, so could not be compared for simulations with a beta error. Some outliers where `decon` produced a large ISE are truncated from these plots. No P-MLE results have been truncated.

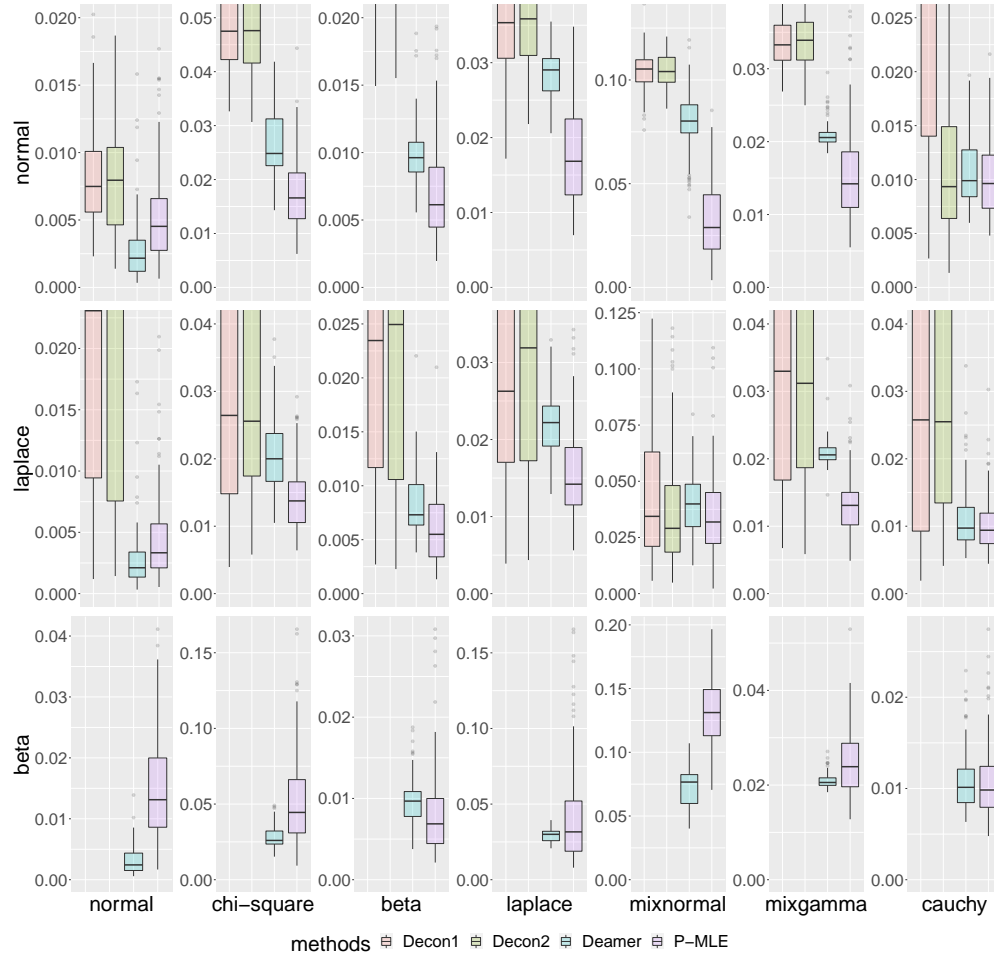


Figure S6: Sample distribution of ISE for sample size 300 and SNR 4. Each column corresponds to one of the seven true distributions in the simulation. Rows correspond to the error distribution. The `decon` package only allows a limited selection of error families, so could not be compared for simulations with a beta error. Some outliers where `decon` produced a large ISE are truncated from these plots. No P-MLE results have been truncated.

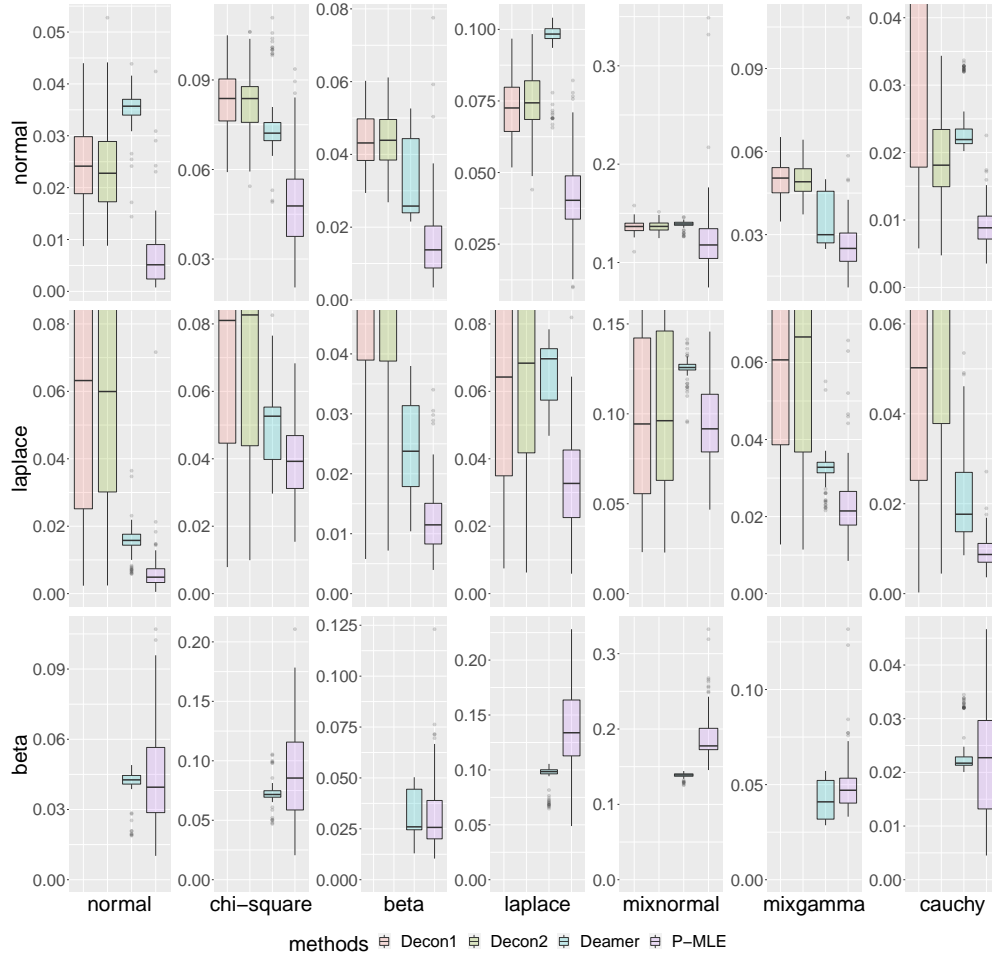


Figure S7: Sample distribution of ISE for sample size 300 and SNR 1. Each column corresponds to one of the seven true distributions in the simulation. Rows correspond to the error distribution. The `decon` package only allows a limited selection of error families, so could not be compared for simulations with a beta error. Some outliers where `decon` produced a large ISE are truncated from these plots. No P-MLE results have been truncated.

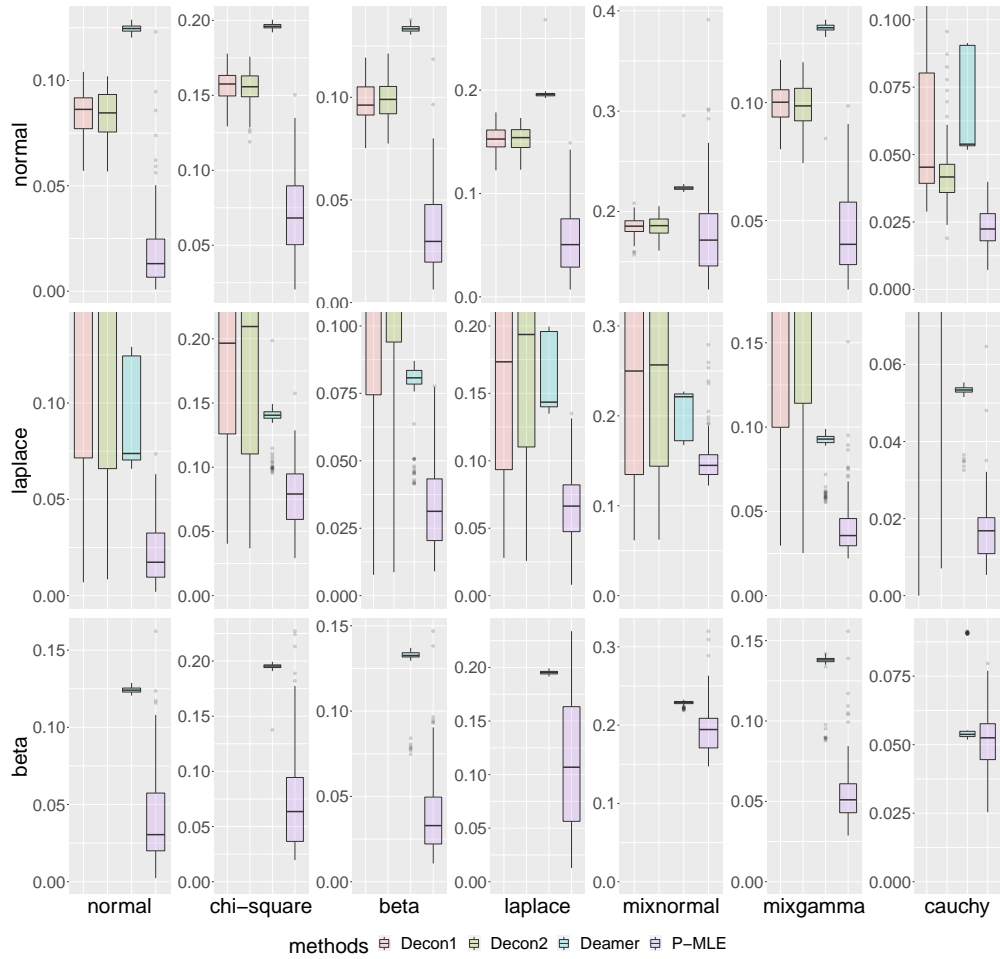


Figure S8: Sample distribution of ISE for sample size 300 and SNR 0.25. Each column corresponds to one of the seven true distributions in the simulation. Rows correspond to the error distribution. The `decon` package only allows a limited selection of error families, so could not be compared for simulations with a beta error. Some outliers where `decon` produced a large ISE are truncated from these plots. No P-MLE results have been truncated.

Table S1: Simulation Results for some Scenarios with different heuristic values for λ_n .

Significantly better results are highlighted in yellow. Results that are not significantly different are highlighted in orange.

Scenario		n	C	Best Heuristic λ_n	Old MISE (SE)	New MISE (SE)	Deamer MISE	Decon MISE
Truth	Error							
cauchy	normal	30	0.5	1,000	0.0380(0.0080)	0.0294(0.0012)		0.0368(0.0010)
mixnormal	beta	100	1	10,000,000	0.2095(0.0063)	0.1670(0.0054)	0.1679(0.0054)	
mixgamma	beta	100	1	1,000,000	0.0614(0.0029)	0.0506(0.0032)	0.0505(0.0014)	
normal	laplace	300	2	100,000	0.0046(0.0004)	0.0028(0.0002)	0.0029(0.0003)	
chi-squared	beta	300	1	10,000,000	0.0895(0.0038)	0.0800(0.0048)	0.0724(0.0010)	
mixgamma	beta	300	1	10,000,000	0.0503(0.0016)	0.0410(0.0015)	0.0420(0.0010)	
laplace	beta	300	1	100,000	0.1361(0.0037)	0.1010(0.0034)	0.0946(0.0010)	
normal	beta	300	1	10,000,000	0.0431(0.0021)	0.0345(0.0012)	0.0411(0.0006)	
beta	beta	300	1	10,000,000	0.0316(0.0018)	0.0250(0.0019)	0.0311(0.0010)	